DISASTER PREVENTION RESEARCH INSTITUTE
BULLETIN No. 26 OCTOBER, 1958

ON THE RHEOLOGICAL CHARACTERS OF CLAY
PART 1

BY

SAKURŌ MURAYAMA
AND
TŌRU SHIBATA

KYOTO UNIVERSITY, KYOTO, JAPAN

DISASTER PREVENTION RESEARCH INSTITUTE
KYOTO UNIVERSITY
BULLETINS

Bulletin No. 26 October, 1958

On the Rheological Characters of Clay
Part 1

By

Sakurō MURAYAMA and Tōru SHIBATA

Contents

Synopsis

This is one part of the report* of a theoretical research on the rheological properties of clay. In this paper, the authors indicate that the representation of clay by the complex combination of simple mechanical model units causes the complication on the mathematical treatment, but does not always contribute to the analysis of essential nature of clay, and insist that the solution of rheological behaviour of clay should be treated with the theory deduced from the micrometric standpoint.

From this standpoint, applying the structural viscosity derived from the statistical mechanics on viscosity of clay, a new fundamental formula concerning the deformation or strength characters of clay—such as flow or long-term strength is derived. This formula well agrees with the various kinds of experiments—experiments on compression flow, recovery, flow by repetitional load, yielding, failure, etc.. Furthermore, results of tests on flow, yielding, failure or thermal effect can be explained micrometically by this formula.

Applying the formula and experiments, some important problems on soil structure—such as strength~water content relation, relation between yielding valure and failure strength, time lapse necessary for failure, variation in strength by flow—are investigated and a new measuring method of yielding value of clay is proposed.

Introduction

This is a report on the rheological characters of clay theoretically researched from the micrometric standpoint.

Formerly the apparent mechanical behaviour of clay was represented frequently by the behaviour of the complex combination of simple mechanical model units such as dashpots, springs or sliders. But the real character of clay is too much complicated to be represented by such a simple model analogy. Moreover, this method of representation dose not always contribute to the analysis of the essential character of clay behaviour in spite of its com-

---

* This is an English report translated from one part of the Transactions of Japanese Society of Civil Engineers No. 40 published in Dec. 1956.

plicated mathematical treatment. Therefore the authors believe that the solution of the rheological behaviour of clay should be treated with the theory deduced from the micrometric standpoint considering the structure of clay.

From this standpoint, in this paper, the rheological characters of clay are researched, and the contents of the research are as follows :

In chapter 1, applying the structural viscosity derived from the statistical mechanics on viscosity of clay, a new fundamental formula concerning the flow character of clay is derived.

Chapter 2 is a report on the experimental results and their considerations of a series of compression flow tests of clay to refer and ascertain the formula derived in Chapter 1. Any flow characters of clay in the experiments exactly agree with the formula so far as the intensity of applied flow stress is less than either the pre-consolidation pressure or the upper yield value.

In Chapter 3, some important problems on soil strength—such as the relations between clay strength and its water content, relation between failure strength and the time lapse necessary for failure and variation in strength by flow—are researched theoretically and experimentally and a new measuring method of the yield value of clay is proposed.

In this report rheological terms are used following the International Rheological Nomenclature[1] ; for instance, the time effect of the deformation of clay is called "flow" but not "creep", because the latter term implies complete recovery.

Chapter 1 The Flow Mechanism of Clay

1. Introduction

In this chapter, the fundamental relation of strain character of clay under constant external stress, that is, the flow character of clay is deduced from the micrometric standpoint applying following 3 assumptions.

(1) The viscosity of clay exerting on the flow of clay is assumed as the structural viscosity which is derived by applying the statistical mechanics on the frequency of the mutual exchange of position between a clay particle and the neighbouring hole or the point of irregularity in the arrangement of particles (c.f. Fig. 1.1).

(2) The mechanical model of clay is assumed from the consideration on the structure of clay as the model as shown in Fig. 1.3 which consists of the

modified Voigt element with series coupling of spring E_1. The coefficient of viscosity η_2 in the modified Voigt element is represented by the structural viscosity deduced from (1). The modified Voigt element, therefore, is composed of a spring element E_2, a dashpot element η_2 and a slider element σ_0 connected in parallel coupling each other whose elastic modulus, coefficient of viscosity and restraining resistance are E_2 (=constant), η_2 (=coefficient of structural viscosity deduced from (1)) and σ_0 (=constant) respectively.

(3) The fundamental relation of flow of clay obtained applying above assumption is supposed to be valid so far as the external stress applied on clay is less than either the stress of pre-consolidation or the stress which breaks the structure of clay.

The structural viscosity of clay which was deduced in this paper may be said to be a extention of the viscosity deduced by H.Eyring. Thus obtained formula will be ascertained with experiments in Chapter 2, and the results of this formula exactly agree with the experimental results of Chapter 2.

2. Structural Viscosity proposed by the Authors

Before the structural viscosity proposed by the authors is explained, it would be convenient to explain about A.V.Tobolsky and H.Eyring's theory,[2] which is founded on the concept that the flow process of polymeric material is produced by exchange of positions between particles and their neighbouring holes. Such a set of a particle and its neighbouing hole which exchange their positions is called a unit process of deformation.

The detailed mechanism considered by Eyring[3] in his rate process theory is depicted in Fig. 1.1. Since the point of irregularity in the arrangement of the particles can be cosidered as the hole, the exact size and shape of which need not be known in advance. The flow process is then considered to be the jump of a particle which is denoted by (a) in Fig. 1.1 from its potential energy well into a neighbouring hole by (b), that is, from one equilibrium position to the next.

In the absence of external stress, forward and backward jumps will be equally frequent. Eyring obtained by statistical mechanics the following expression for this jump frequency J:

$$J=\frac{\kappa T}{h}\exp\left(\frac{-E_0}{\kappa T}\right)$$

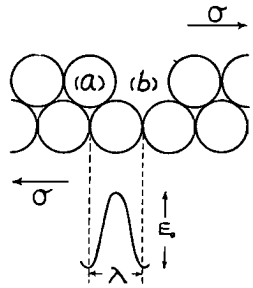

Fig. 1.1 Schematic sketch of the structure composed of particles and holes

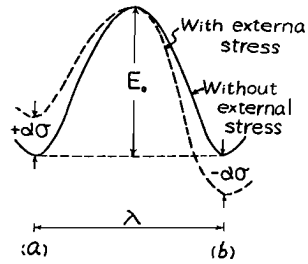

Fig. 1.2 Representation of potential energy barrier with or without external stress

Where κ is Boltzmann's constant, T is the absolute temperature, h is Planck's constant and E_0 is the free energy of activation for the jump, that is the potential energy barrier as shown in Fig. 1.1. In the presence of a shearing stress σ the potential barrier will be deformed so as to favour the forward jumps as shown in Fig. 1.2., i.e., the potential barrier is biased in the direction of motion by the amount $-a\sigma$ and by the same amount with opposite sign in the backward direction. Therefore the net frequency of jump or the net rate of motion should be represented as

$$\frac{\kappa T}{h}\exp\left\{\frac{-(E_0-a\sigma)}{\kappa T}\right\}-\frac{\kappa T}{h}\exp\left\{\frac{-(E_0+a\sigma)}{\kappa T}\right\}$$
$$=\frac{2\kappa T}{h}\exp\left(\frac{-E_0}{\kappa T}\right)\sinh\left(\frac{a\sigma}{\kappa T}\right) \tag{2.1}$$

where $a=\lambda/2N$, and λ is the average distance projected in the direction of stress between equilibrium positions and N is the number of unit process of deformation in a unit area of cross section perpendicular to the direction of stress. And also, if there are n unit of processes of deformation in series per unit length in the direction of stress, the rate of shear D should be

$$\left.\begin{aligned} D&=C\exp\left(\frac{-E_0}{\kappa T}\right)\sinh\left(\frac{a\sigma}{\kappa T}\right)\\ C&=\frac{2\lambda n\kappa T}{h}\end{aligned}\right\} \tag{2.2}$$

The equation for the apparent viscosity coefficient of flow would then become

$$\eta=\frac{\sigma}{D}=\frac{1}{C}\exp\left(\frac{E_0}{\kappa T}\right)\frac{\sigma}{\sinh\left(\frac{a\sigma}{\kappa T}\right)} \tag{2.3}$$

The most significant result of the Eyring's theory, therefore, is to provide a basis for equation (2.3) which has been employed so successfully to represent the structural viscosity and the viscosity-temperature dependence of ordinary liquids at ordinary temperatures.

In order to represent the rheological behaviour of the material of more complex structure, the more general relationship can be derived by assuming the generalized model of the material which consists of r parallel groups of different types of unit processes of deformation described as follows and by applying the W. Kuhn's theory[4] which gives the stress σ and strain ε of the material as the sum of the each elementary stress σ_i and strain ε_i of the group of unit processes of deformation of type i, thus : $\sigma=\sum_1^r\sigma_i$ and $\varepsilon=\sum_1^r\varepsilon_i$.

In the group of unit processes of deformation of type i, there are N_i units of parallel process of deformation of type i in a unit area of cross section perpendicular to the direction of stress σ_i, and unit stress σ_i distributed on N_i units (viz. the average force acting on each unit is σ_i/N_i), and also there are such n_i unit of processes of deformation of this type in series per unit length in the direction of stress σ_i.

Applying these assumptions to Eyring's theory which is represented by Eq. (2.2), Tobolsky and Eyring led the following equation relating the rate of strain $d\varepsilon_i/dt$ with the stress σ_i.

$$\frac{d\varepsilon_i}{dt}=\frac{2\lambda_i n_i\kappa T}{h}\exp\left(\frac{-E_{0i}}{\kappa T}\right)\sinh\left(\frac{\lambda_i\sigma_i}{2N_i\kappa T}\right)=A_i'\sinh(B_i'\sigma_i)$$

where $$A_i'=\frac{2\lambda_i n_i\kappa T}{h}\exp\left(\frac{-E_{0i}}{\kappa T}\right),\quad B_i'=\frac{\lambda_i}{2N_i\kappa T} \tag{2.4}$$

In the treatment above stated, the number of the unit process of deformation is considered to be independent of applied stress, and does not refer to the existence of restraining resistance against flow which acts on particles at all.

On the solution of rheological behaviour of clay, in this paper, the authors have taken the restraining resistance acting on clay particles in consideration and further have assumed that N_i or n_i varies with a function of total stress (σ) applied on the clay skeleton. Consequently, the unit process

of deformation is restrained to participate in deformation until the total stress overcomes the restraining stress σ_0, and when σ become greater than σ_0, it is assumed that the number of unit processes of deformation which participate in deformation increase in direct proportion to the value of $(\sigma-\sigma_0)$. The latter assumption is based on the consideration that no special regularity in the arrangement of clay particles is expected.

Hence, the above assumption can be expressed in the following equations.

$$\left.\begin{array}{ll} \text{where} \quad 0<\sigma<\sigma_0 & n_i \text{ or } N_i=0 \\ \sigma_0<\sigma & n_i=a(\sigma-\sigma_0) \\ & N_i=b(\sigma-\sigma_0) \end{array}\right\} \tag{2.5}$$

where a and b are constants respectively.

On the basis of above assumptions, the frequency of forward jump j_+ should be

$$j_+=\frac{\kappa T}{h}\exp\left\{\frac{-\left(E_{0i}-\dfrac{\lambda_i\sigma_i}{2b(\sigma-\sigma_0)}\right)}{\kappa T}\right\} \tag{2.6}$$

and the frequency of backward jump j_- should be

$$j_-=\frac{\kappa T}{h}\exp\left\{\frac{-\left(E_{0i}+\dfrac{\lambda_i\sigma_i}{2b(\sigma-\sigma_0)}\right)}{\kappa T}\right\} \tag{2.7}$$

where E_{0i} is the free energy of activation of the unit process of deformation of type i.

Therefore the net rate of jump should be

$$j=j_+-j_-=\frac{2\kappa T}{h}\exp\left(\frac{-E_{0i}}{\kappa T}\right)\sinh\left\{\frac{\lambda_i\sigma_i}{2b\kappa T(\sigma-\sigma_0)}\right\} \tag{2.8}$$

Corresponding to Eq. (2.4), we obtain the following equation between the rate of strain $d\varepsilon_i/dt$ and the stress σ_i.

$$\begin{aligned}\frac{d\varepsilon_i}{dt}&=\frac{2\lambda_i a(\sigma-\sigma_0)\kappa T}{h}\exp\left(\frac{-E_{0i}}{\kappa T}\right)\sinh\left\{\frac{\lambda_i\sigma_i}{2b\kappa T(\sigma-\sigma_0)}\right\}\\&=A_i(\sigma-\sigma_0)\sinh\left(\frac{B_i\sigma_i}{\sigma-\sigma_0}\right)\end{aligned} \tag{2.9}$$

where $$A_i=\frac{2\lambda_i a\kappa T}{h}\exp\left(\frac{-E_{0i}}{\kappa T}\right), \qquad B_i=\frac{\lambda_i}{2b\kappa T}$$

Hence, for the unit process of deformation of type i, the apparent coefficient of viscosity proposed by the authors is represented as

$$\eta_i=\frac{1}{A_i\sinh\left(\dfrac{B_i\sigma_i}{\sigma-\sigma_0}\right)} \tag{2.10}$$

3. Mechanical Model and Flow Mechanism of Clay

As the results of many preparatory tests on clay, it has been observed that the clay behaves visco-elastically but has a lower yield value corresponding to the restraining resistance, below which no flow deformation can be detected. From these test results and following consideration, the authors adopt a special model as the mechanical model of clay. This special model, as shown in Fig. 1.3, consists of a series coupling of a spring element E_1 whose elastic modulus is E_1 and a modified Voigt element composed of a spring element E_2, a dashpot element η_2 and slider element σ_0 connected in parallel position each other, whose elastic modulus, coefficient of viscosity and restraining resistance are E_2, η_2 and σ_0 respectively. The coefficient of viscosity η_2 of the Voigt element is represented by the structural viscosity expressed in Eq. (2.10).

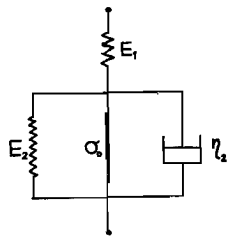

Fig. 1.3 Mechanical model representing clay skeleton

On the construction of the above mechanical model, the following consideration may be applied. Structure of clay is supposed as it is composed of aggregates of matrices accumulatively composed of very fine fractions, so that the elastic properties E_1 must be ascribed to the elastic repulsion between matrices as if elasticity of sand mass is caused by the elasticity between sand grains in it. On the other hand, as the application of external force causes the exchange of positions between particles and neighbouring holes in the matrix, clay shows the structural viscosity η_2 on the flow process.

Although the frequency or the number of activating unit process of deformation per unit time may change accordance with $(\sigma-\sigma_0)$, it may be supposed that the total existing number of unit process of deformation in the matrix is unchanged independent of the magnitude of external stress so far as the external stress is less than the stress which breaks the structure of the matrix, because the flow process of clay is only caused by the mutual exchange of positions between particles and holes in the matrix so far as the external stress is less than the pre-consolidation stress. Since the elastic property of the matrix, furthermore, is supposed to be dependent of the elastic property of the part of the matrix in which no unit process of deformation exists, the elastic modulus E_2 of the matrix is assumed to be constant in spite

of the magnitude of external stress.

From Eq. (2.9) and (2.10), the strain rate $d\varepsilon_2/dt$ and the apparent coefficient of viscosity η_2 for this mechanical model are given as follows.

$$\frac{d\varepsilon_2}{dt}=A_2(\sigma-\sigma_0)\sinh\left(\frac{B_2\sigma_2}{\sigma-\sigma_0}\right) \tag{3.1}$$

$$\eta_2=\frac{1}{A_2\sinh\left(\frac{B_2\sigma_2}{\sigma-\sigma_0}\right)} \tag{3.2}$$

where ε_2 is strain of modified Voigt model and σ_2 is applied stress on the dashpot η_2. The relation between total strain ε and time t, can be obtained by solving the following simultaneous equations,

$$\begin{cases}\varepsilon=\varepsilon_1+\varepsilon_2 & (3.3)\\ \sigma=\varepsilon_1E_1 & (3.4)\\ \sigma=\varepsilon_2E_2+\dfrac{(\sigma-\sigma_0)}{B_2}\sinh^{-1}\left\{\dfrac{1}{A_2(\sigma-\sigma_0)}\dfrac{d\varepsilon_2}{dt}\right\}+\sigma_0 & (3.5)\end{cases}$$

Transformation of Eq. (3.5) leads to:

$$\frac{d\varepsilon_2}{dt}=A_2(\sigma-\sigma_0)\sinh\left[\frac{B_2\{(\sigma-\sigma_0)-\varepsilon_2E_2\}}{(\sigma-\sigma_0)}\right]$$

Integrating, we obtain

$$\int\frac{d\varepsilon_2}{\sinh\left[\frac{B_2\{(\sigma-\sigma_0)-\varepsilon_2E_2\}}{(\sigma-\sigma_0)}\right]}=A_2(\sigma-\sigma_0)\int dt+C$$

from which

$$-\frac{(\sigma-\sigma_0)}{B_2E_2}\log\tanh\left[\frac{B_2\{(\sigma-\sigma_0)-\varepsilon_2E_2\}}{2(\sigma-\sigma_0)}\right]=A_2(\sigma-\sigma_0)t+C \tag{3.6}$$

The arbitrary constant C is equal to $C=-\dfrac{(\sigma-\sigma_0)}{B_2E_2}\log\tanh\left(\dfrac{B_2}{2}\right)$, since we have $\varepsilon_2=0$ at $t=0$.

Substituting this constant into Eq. (3.6), we obtain

$$\log\tanh\left[\frac{B_2\{(\sigma-\sigma_0)-\varepsilon_2E_2\}}{2(\sigma-\sigma_0)}\right]=-A_2B_2E_2t+\log\tanh\left(\frac{B_2}{2}\right) \tag{3.7}$$

From Eq. (3.7) we get the relation between ε_2 and t

$$\varepsilon_2=\frac{(\sigma-\sigma_0)}{E_2}-\frac{2(\sigma-\sigma_0)}{B_2E_2}\tanh^{-1}\left\{\exp(-A_2B_2E_2t)\tanh\left(\frac{B_2}{2}\right)\right\} \tag{3.8}$$

If $B_2/2$ is larger than unity and

$$2B_2>\frac{2B_2\{(\sigma-\sigma_0)-\varepsilon_2E_2\}}{(\sigma-\sigma_0)}>1$$

or

$$0<\varepsilon_2<\frac{(\sigma-\sigma_0)}{2B_2E_2}(2B_2-1) \tag{3.9}$$

approximate result is given as

$$\log\tanh\left[\frac{B_2\{(\sigma-\sigma_0)-\varepsilon_2E_2\}}{2(\sigma-\sigma_0)}\right]-\log\tanh\left(\frac{B_2}{2}\right)$$

$$=\log\left[1-2\exp\left[\frac{-B_2\{(\sigma-\sigma_0)-\varepsilon_2E_2\}}{(\sigma-\sigma_0)}\right]+2\exp\left[\frac{-2B_2\{(\sigma-\sigma_0)-\varepsilon_2E_2\}}{(\sigma-\sigma_0)}\right]-\cdots\cdots\right]$$

$$-\log\left[1-2\exp(-B_2)+2\exp(-2B_2)-\cdots\cdots\right]$$

$$\fallingdotseq\log\left[1-2\exp\left[\frac{-B_2\{(\sigma-\sigma_0)-\varepsilon_2E_2\}}{(\sigma-\sigma_0)}\right]+2\exp\left[\frac{-2B_2\{(\sigma-\sigma_0)-\varepsilon_2E_2\}}{(\sigma-\sigma_0)}\right]-\cdots\cdots\right]$$

$$\fallingdotseq-2\exp\left[\frac{-B_2\{(\sigma-\sigma_0)-\varepsilon_2E_2\}}{(\sigma-\sigma_0)}\right]$$

Accordingly,

$$-2\exp\left[\frac{-B_2\{(\sigma-\sigma_0)-\varepsilon_2E_2\}}{(\sigma-\sigma_0)}\right]=-A_2B_2E_2t \tag{3.10}$$

then, strain of modified Voigt element ε_2 will be

$$\varepsilon_2=\frac{(\sigma-\sigma_0)}{E_2}+\frac{(\sigma-\sigma_0)}{B_2E_2}\log A_2'B_2E_2t \tag{3.11}$$

where $A_2'=A_2/2$.

Substituting Eq. (3.11) into Eq. (3.3), we obtain

$$\varepsilon=\frac{\sigma}{E_1}+\frac{(\sigma-\sigma_0)}{E_2}+\frac{(\sigma-\sigma_0)}{B_2E_2}\log A_2'B_2E_2+\frac{(\sigma-\sigma_0)}{B_2E_2}\log t \tag{3.12}$$

Eq. (3.12) is the "flow equation" representing the relation between strain ε and time t for the condition (3.9), and in this equation ε is proportional to $\log t$.

If ε_2 beyonds the limits of (3.9), viz.

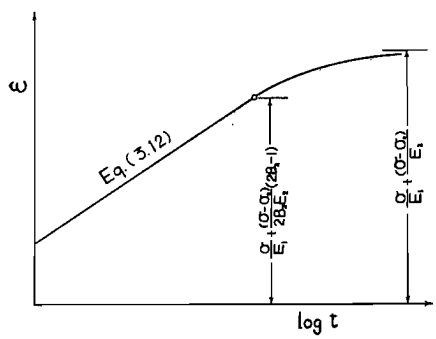

Fig. 1.4 Schematic diagram of flow strain ε vs. time t

$$\varepsilon_2>\frac{(\sigma-\sigma_0)}{2B_2E_2}(2B_2-1) \tag{3.13}$$

Eq. (3.8) becomes

$$\varepsilon_2=\frac{(\sigma-\sigma_0)}{E_2} \tag{3.14}$$

at $t\to\infty$.

Substituting Eq. (3.14) into Eq. (3.3), we obtain

$$\varepsilon_{t\to\infty}=\frac{\sigma}{E_1}+\frac{(\sigma-\sigma_0)}{E_2} \tag{3.15}$$

According to the theory proposed by the authors, therefore,

the curve representing the relation between the strain of clay and the logarithm of the loading time should approach to a horizontal asymptote as shown schematically in Fig. 1.4.

Chapter 2 Studies on the Flow Tests

4. Introduction

In this chapter, the authors report on the experimental results and their considerations of a series of compression tests at constant uni-axial load, carried out on Osaka Alluvial Clay, in order to refer and ascertain the new fundamental formula derived in the preceding chapter.

As the experimenting apparatus for flow tests of clay, there are various kinds of apparatus such as apparatus for simple shear, torsion shear, unconfined compression, triaxial compression or other testing method and some of them have been used by some researchers. But, in this case, for simplicity and general applicability of testing process, the authors performed the compression flow tests with triaxial cell applying each constant uni-axial load, as R.Haefeli[6] performed.

5. Some Data of the Clay Specimen and the Compression Plastometer

Undisturbed clay specimens used for the compression flow tests were obtained from the Umeda Alluvial Clay Stratum in Osaka City by means of the thin-walled sampler with stationary piston. The tube of this sampler has the inner diameter of 73 mm, the thickness of the wall of about 1 mm and the length of 760 mm. The soil profile of the Osaka Alluvial Layer is shown in Fig. 2.1, in which clay stratum extending between a depth from 6 to 18 m below ground level is called Umeda Alluvial Clay Stratum. As the clay in this stratum has the sensitivity ratio of about 3 in Terzaghi's representation, it belongs to the category of an ordinary clay. The results of the physical tests of the clay are as follows : — specific gravity : 2.67, L.L. ; 83~63%, P.L. ; 36~25%, natural water content : 92~58%, void ratio : 2.52~1.84, degree of saturation : 100%, and the grain size distribution is shown in Fig. 2.2. The maximum pre-consolidation pressures measured by oedometer tests are as follows : — sample No. 4 ; 0.88 kg/cm^2, No. 10 ; 1.60 kg/cm^2. As

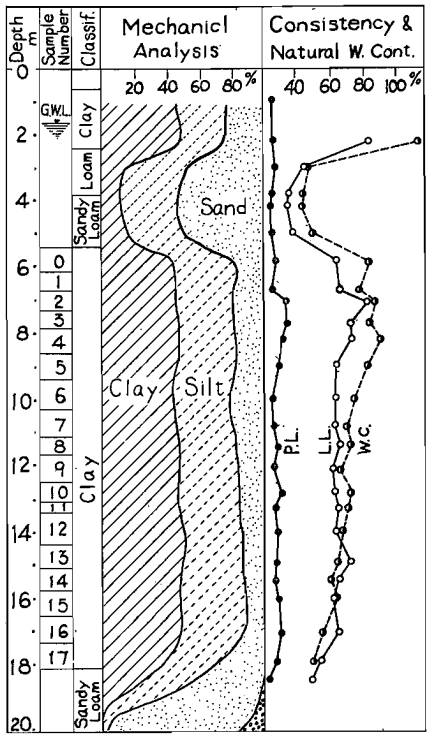

Fig. 2.1 Soil profile of the Osaka Alluvial Clay

these pre-consolidation pressures are equal to their overburden pressures respectively, the clay in this stratum is normally loaded clay.

In the case of the compression flow tests, a triaxial compression apparatus was used as compression plastometer. In these tests, a constant uni-axial load was applied on the clay specimen in a triaxial apparatus whose schematic appearance is illustrated in Fig. 2.3, where the clay specimen is denoted by A, the pressure chamber B, the loading lever (lever ratio ; 1/10) by C and the dialgauge by D. The clay specimen was obtained by shaven out from the undisturbed sample to have a cylindrical form with a height of $h=8.0$ cm and a diameter of 3.5 cm. On the compression test, longitudinal displacement Δh (mm) of clay specimen was measured by the dialgauge. Then the strain ε is given by $\Delta h/h$ so far as

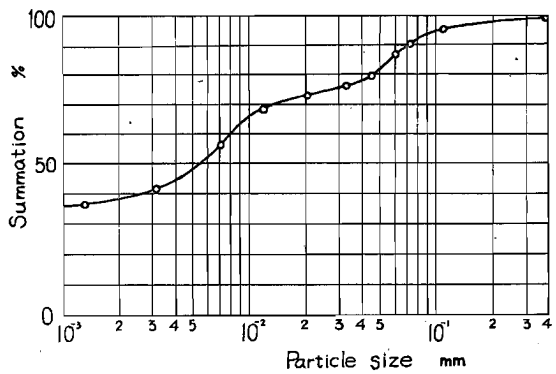

Fig. 2.2 Grain size distribution curve

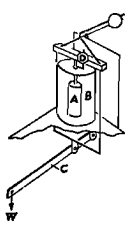

Fig. 2.3 Schematic appearance of compression plastometer

displacement is assumed to be infinitesimal.

In these tests, compression loads were so restrained as the vertical stresses σ in the specimens to be less than the pre-consolidation pressures to avoid the effect of consolidation. On a series of compression flow tests, to avoid the effects of the stress-history given to the specimen by the compression test, each "fresh specimen" obtained from a same clay sample which had never received any compression test was used for each constant uni-axial load. To protect from the evaporation at the surface of the clay specimen, the specimen was coated by grease and covered by thin gum membrane and the pressure chamber was filled by water for the duration of the tests.

6. Flow Characteristics

Using clay samples above stated, compression flow tests were performed in which stress is kept as constant as possible during the tests of 24 hrs. The results of the tests are shown as strain~time diagrams in Fig. 2.4, 2.5 and 2.6, in which each abscissa shows elapsed time t in logarithmic scale and each ordinate strain ε respectively.

From the strain~time curves, the features worth noticing are as follows.

(1) The flow strain ε increases proportionally to the logarithm of time $(\log t)$[6][7], if the applied stress σ is smaller than a certain critical value.

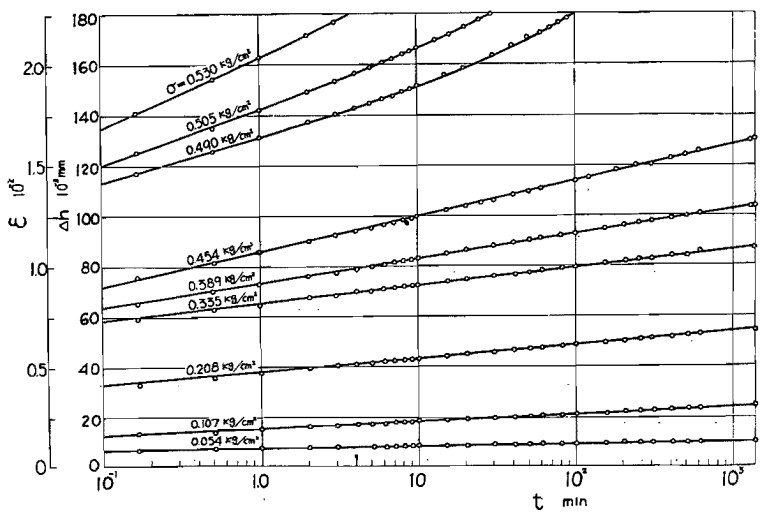

Fig 2.4 Flow strain ε vs. time t curves (sample No. 13, water content ; 65%)

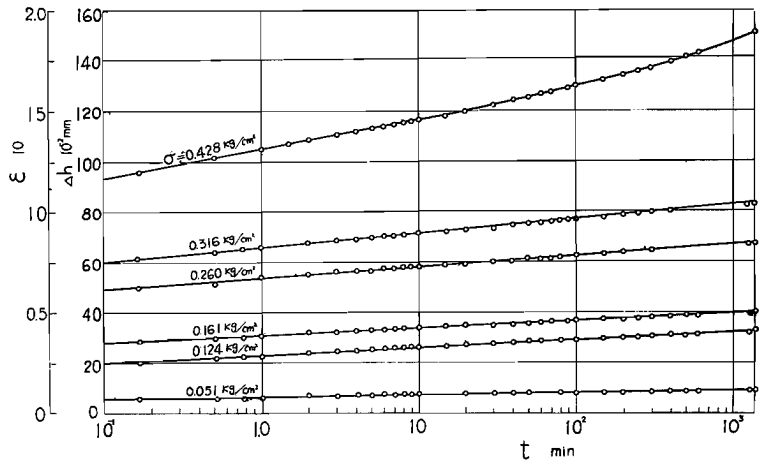

Fig. 2.5 Flow strain ε vs. time t curves (sample No. 8, water content ; 75%)

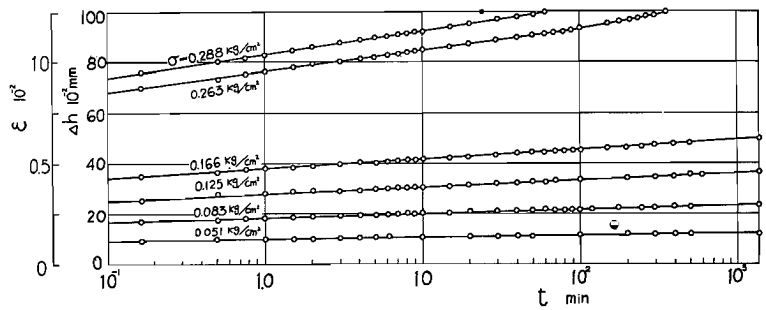

Fig. 2.6 Flow strain ε vs. time t curves (sample No. 4, water content ; 92%)

Therefore, it may be confirmed that Eq. (3.12) representing the linear relation between the flow strain and the logarithm of time is valid for the stress range up to a certain critical value.

(2) If the applied stress is larger than a certain critical value, the curves in these figures rise concave upwards and this tendency suggests the occurence of failure in future after a certain duration.

It will be discussed in the following Article 7 that each critical value coincides with the upper yield value.

(3) The slopes of these lines related in (1) increase with applied stresses, and it will be showed that the tangent of the slope angle of each line is directly proportional to the applied stress as shown in Fig. 2.7 whose ordinate

and abscissa show the tangent of the slope angle of the line and the applied stress of the curve illustrated in Fig. 2.4, 2.5 and 2.6 respectively.

7. Strain-rate Characteristics

In this article, the effects of stress σ or time t on strain-rate $d\varepsilon/dt$ are analysed.

From Eq. (3.12) the strain-rate can be represented as

$$\frac{d\varepsilon}{dt}=\frac{(\sigma-\sigma_0)}{B_2E_2}\frac{1}{t} \qquad (7.1)$$

Taking the logarithm of each term, we get

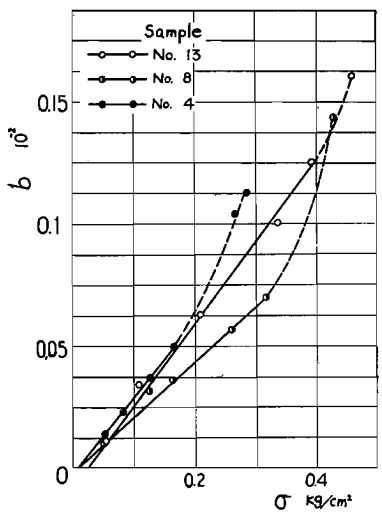

Fig. 2.7 Relations between the coefficient b and applied stress σ

$$\log\left(\frac{d\varepsilon}{dt}\right)=\log\frac{(\sigma-\sigma_0)}{B_2E_2}-\log t \qquad (7.2)$$

On the other hand, Eq. (3.12) is transformed :

$$\varepsilon=\frac{\sigma}{E_1}+\frac{(\sigma-\sigma_0)}{E_2}+\frac{2.3(\sigma-\sigma_0)}{B_2E_2}\log_{10}A_2'B_2E_2t \qquad (7.3)$$

$$=a+b\log_{10}t \qquad (7.4)$$

where $$a=\frac{\sigma}{E_1}+\frac{(\sigma-\sigma_0)}{E_2}+\frac{2.3(\sigma-\sigma_0)}{B_2E_2}\log_{10}A_2'B_2E_2$$

$$b=\frac{2.3(\sigma-\sigma_0)}{B_2E_2}$$

From the above treatment on strain-rate equations (7.1) and (7.2), the following characters of strain-rate can be presumed so far as the flow of clay are ruled by the theory stated in Article 3.

(1) The relation between strain-rate and stress for various constant values of the time is represented by straight line.

(2) The logarithmic relation between strain-rate at a constant stress and time is represented by straight lines.

These characters of strain-rate are ascertained as follows from the experimental results on flow of clay shown in Fig. 2.4, 2.5 and 2.6.

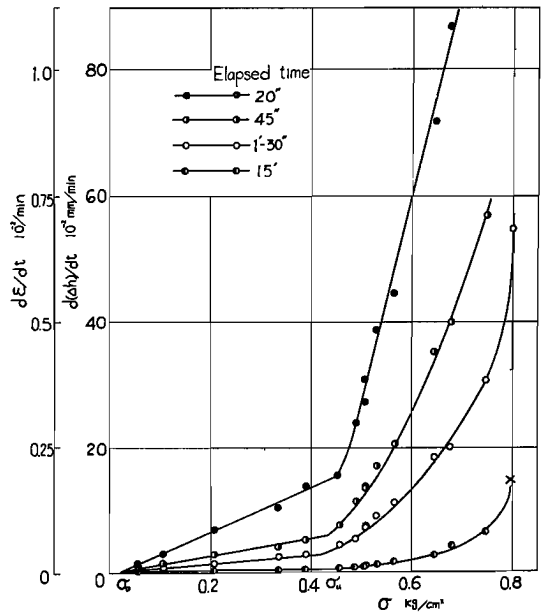

Fig. 2.8 Viscosity characteristic (sample No. 13)

The consideration for (1) :

In Fig. 2.8 the strain-rate $d\varepsilon/dt$ obtained from Fig. 2.4 (in the case of clay sample of No. 13) is plotted against the applied stress σ for various constant values of the time, taking the time as $t=20$ sec, 45 sec, 1.5 min and 15 min. This figure shows that the curves are linear within the stress range up to $\sigma=0.45$ kg/cm², whereas they rise concave upwards at $\sigma>0.45$ kg/cm². Moreover all linear parts of these curves concentrate at a point on the σ-axis. The abscissa of the point of intersection of these lines with the σ-axis is called the lower yield value σ_0, below which the strain-rate equals to zero and no flow deformation takes place. The stresses corresponding to the points of first inflection of curves or the upper end points of linear parts are equal for every lines and this stress is called the upper yield value σ_u, below which no failure can occur even after long periods of time elapsed. Thus the lower and upper yield values can be uniquely determined by strain-rate~stress diagram as shown in Fig. 2.8 which corresponds to so-called $D\sim\tau$ relationships or viscosity curves. As above stated, therefore, the part of the curves between σ_0 ($=0.025$ kg/cm²) and σ_u ($=0.45$ kg/cm²) are straight lines and within this range Eq. (7.1) is valid.

From the same experimental viscosity curves as Fig. 2.8 obtained for samples No. 4 and No. 8, we get the values of σ_0 and σ_u, which are shown in Table 2.1. Within the stress ranges up to the upper yield values tabulated in Table 2.1, the $\varepsilon \sim \log t$ relations of these clay samples under a constant uni-axial stress are linear as shown in Fig. 2.4, 2.5 and 2.6, and in these ranges of stress Eq. (3.12) is valid.

Table 2.1

Sample No.	σ_0 kg/cm^2	σ_u kg/cm^2
13	0.025	0.45
8	0.020	0.33
4	0.020	0.19

The thick lines in Fig. 2.7 show the relations between the coefficient of b in Eq. (7.4) and the applied stress σ. The value of b, in this figure, was obtained as the tangent of the slope angle of each straight line due to the comperssion stress smaller than the upper yield value σ_u in Fig. 2.4, 2.5 and 2.6. Since the experimental data lie in well agreement on thick straight lines representing the $b \sim \sigma$ relations for stresses smaller than the upper yield value, it can be said that the value of B_2E_2 in Eq. (7.4) does not depend on stress within the range up to the upper yield value. Therefore, the values of B_2E_2 can be computed from Eq. (7.4) and the results of calculations are shown in Table 2.2.

Table 2.2

Sample No.	B_2E_2 10^3 kg/cm^2	Water content %	Temperature °C
13	0.688	65	22.4
8	1.000	75	2.7
4	0.712	92	2.7

The value of B_2E_2 which influences the strain-rate depends on a large extent on the water content, temperature and other factors of the testing procedure. If we consider the effect of temperature on the value of B_2, it may be presumed that B_2 decreases with increasing absolute temperature, because B_2 is represented as $B_2 = \lambda_2/2b\kappa T$ in Eq. (2.9). The dotted lines in Fig. 2.7 show the relations between the tangents of slope angle of tangent

lines on each curve for the part of $\sigma > \sigma_u$ at $t=1$ min in Fig. 2.4, 2.5 and 2.6 and applied stress σ. These dotted lines do not hold linear relation as thick lines do in Fig. 2.7.

The consideration for (2) :

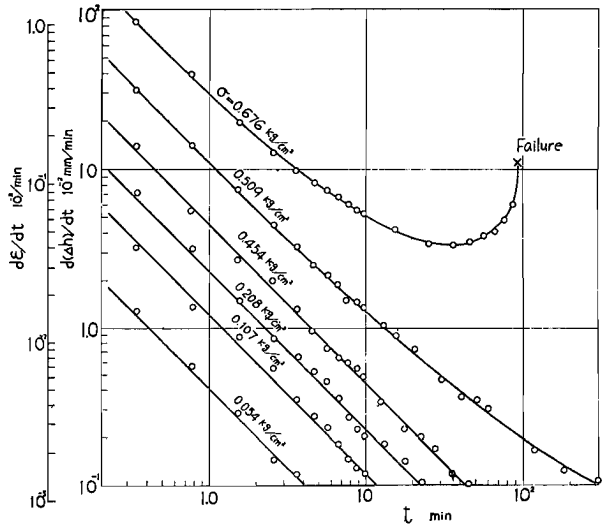

Fig. 2.9 Strian rate $d\varepsilon/dt$ vs. time t curves (sample No. 13)

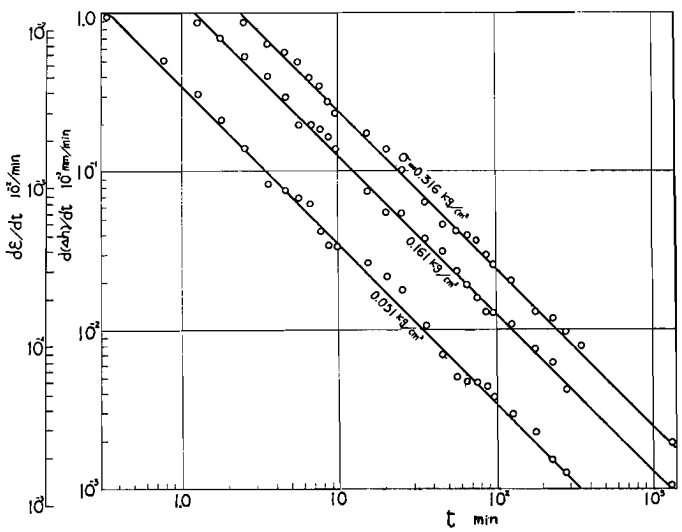

Fig. 2.10 Strain rate $d\varepsilon/dt$ vs. time t curves (sampel No. 8)

Fig. 2.9 and 2.10 show the logarithmic relations between the strain-rate $d\varepsilon/dt$ and time t obtained from the strain~time curves in Fig. 2.4 and 2.5 respectively. The straight lines in these figures represent Eq. (7.2) computed by using the values of B_2E_2 tabulated in Table 2.2. Since the experimental data lie in well agreement on straight lines representing Eq. (7.2) for the stresses smaller than the upper yield values, it can be said that the relation between the strain-rate and the time is quite satisfactory expressed by Eq. (7.2). On the other hand, for stresses larger than the upper yield value the curves rise concave upwards and the failures occur after a certain duration as shown in Fig. 2.9. In this figure, it is found that curves for compression stresses of 0.509 kg/cm^2 and 0.676 kg/cm^2 rise concave upwards and for the curve of 0.676 kg/cm^2 failure occurs after 96 min.

8. Stress~Strain Characteristics

From Eq. (3.12) the strain ε can be represented as

$$\varepsilon=(\sigma-\sigma_0)\left(\frac{1}{E_1}+\frac{1}{E_2}+\frac{1}{B_2E_2}\log A_2'B_2E_2+\frac{1}{B_2E_2}\log t\right)+\varepsilon_0 \tag{8. 1}$$

where $\varepsilon_0=\frac{\sigma_0}{E_1}$

Since ε_0 nearly equals to zero, above equation becomes approximately

$$\varepsilon=(\sigma-\sigma_0)\left(\frac{1}{E_1}+\frac{1}{E_2}+\frac{1}{B_2E_2}\log A_2'B_2E_2+\frac{1}{B_2E_2}\log t\right) \tag{8. 2}$$

This equation shows that ε and $(\sigma-\sigma_0)$ lie in proportional relation if elapsed time t is equal.

From Eq. (8.2), as time-function or stress~strain relation regarding to time, $\phi(t)$ are given as follows.

$$\frac{\varepsilon}{(\sigma-\sigma_0)}=\phi(t)=\left(\frac{1}{E_1}+\frac{1}{E_2}+\frac{1}{B_2E_2}\log A_2'B_2E_2+\frac{1}{B_2E_2}\log t\right) \tag{8. 3}$$

$$=a'+b'\log_{10}t$$

where

$$a'=\frac{1}{E_1}+\frac{1}{E_2}+\frac{2.3}{B_2E_2}\log_{10}A_2'B_2E_2 \tag{8. 4}$$

$$b'=\frac{2.3}{B_2E_2}$$

Refering to Eq. (7.4), the coefficients of a' and b' in Eq. (8.4) are represented as $a'\fallingdotseq a/(\sigma-\sigma_0)$, $b'=b/(\sigma-\sigma_0)$.

In Fig. 2.11(a) and 2.12(a), each stress in Fig. 2.4 and 2.5 is plotted against the strains for various constant values of the time. In these figures values

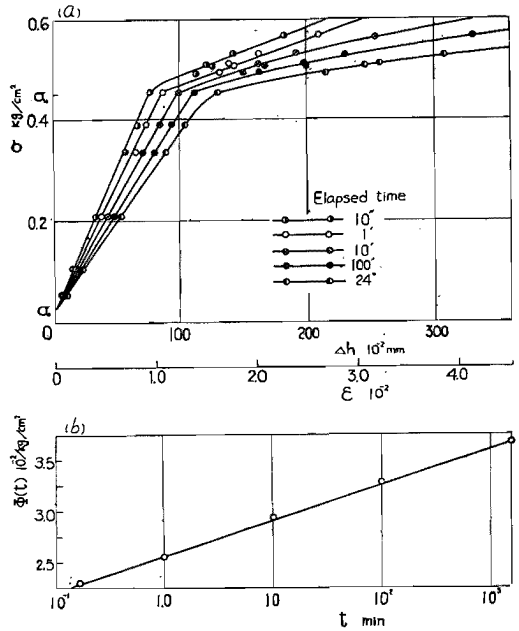

Fig. 2.11 (a) Relations between applied stress σ and strain ε at various instants t (samale No. 13)
(b) Variation of $\phi(t)$ with time

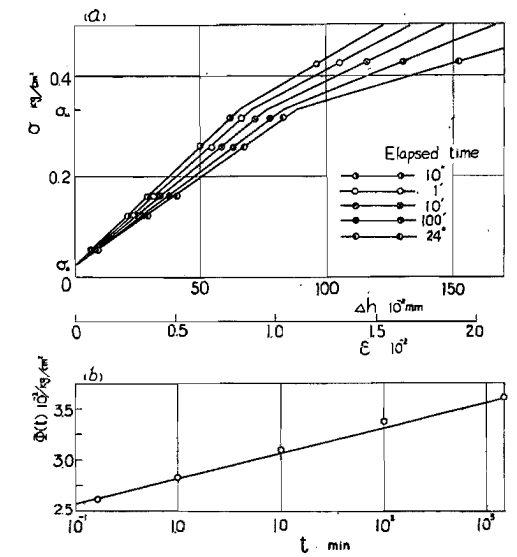

Fig. 2.12 (a) Relations between applied stress σ and strain ε at various instants t (sample No. 8)
(b) Variation of $\phi(t)$ with time

of parameter t are $t=10$ sec, 1, 10, 100 min and 24 hr. All curves concentrate at very near points to the lower yield value σ_0 on σ-axis. The lower part of these curves up to the first inflection points or the upper yield value σ_u are approximately straight lines. Within this range, therefore, Eq. (8.2) is valid and the ratio $\varepsilon/(\sigma-\sigma_0)$ or $\Phi(t)$ plotted against time must give the same time-function $\Phi(t)$. The values of $\Phi(t)$ obtained from Fig. 2.11(a) and 2.12(a) are plotted in Fig. 2.11(b) and 2.12(b).

The experimental results of E.C.W.A. Geuze and T.K. Tan[8] had indicated that $\Phi(t)$ can be uniquely determined from torsional tests at constant moments and further that the time function in simple shear is identical with the time function $\Phi(t)$ in torsion.

The thick lines in Fig. 2.11(b) and 2.12(b) are $\Phi(t)$-lines obtained by the calculation of Eq. (8.4) substituting $a/(\sigma-\sigma_0)$ for a' and B_2E_2 in Table 2.2 for b', and they are represented by each straight line on the semi-logarithmic coordinate system. By above stated calculation, these lines are given as follows;

For Fig. 2.11(b) (for sample No. 13)

$$\Phi(t)=2.65+0.33\log_{10} t \quad 10^{-2}/\mathrm{kg/cm^2}$$

For Fig. 2.12(b) (for sample No. 8)

$$\Phi(t)=2.80+0.23\log_{10} t \quad 10^{-2}/\mathrm{kg/cm^2}$$

As all experimentally obtained plotts of $\Phi(t)$ perfectly lie on the theoretically obtained $\Phi(t)$-lines as shown in Fig. 2.11(b) and 2.12(b), it may be said that the stress~strain characteristics of clay can be deduced from the theory established by the authors and containing elements of time-function $\Phi(t)$ which was introduced as the experimental results by E.C.W.A. Geuze and T.K. Tan[8] are clarified.

9. Characteristics of Flow under Repeated Load and Flow Recovery

In order to get an insight in the flow mechanism of clay, it is of fundamental importance to study the behaviour of the flow strain due to repeated load and flow recovery after the load is taken away. For this purpose, repetitional loads of same magnitude and same loading duration are applied on the clay specimen at same interval of removal of the load according to the method stated in Article 5.

Fig. 2.13(a) and (b) show the schematic relations of the stress~time and the strain~time respectively. The flows and flow recoveries due to the 1st, 2nd,.....and nth loading and load-removing are called the 1st, 2nd,.....and nth flow and flow recovery in this paper.

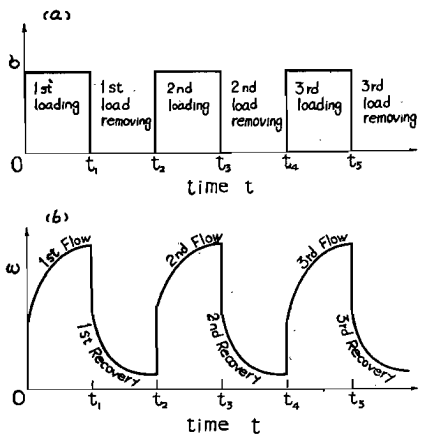

Fig. 2.13 (a) Schematic relations of stress vs. time due to repetitonal loading
(b) Strain vs. time curve due to repetitional loading

Fig. 2.14 and 2.15 show the examples of flow and recovery curves plotted on the semi-logarithmic papers in which the repetitional stresses smaller than the upper yield values were applied as noted in both figures. From the flow and recovery curves in these figures, the following features are noticeable.

(1) The tangent of the slope angle of the 2nd flow curve which is correspondent to the coefficient b in Eq. (7.4) decreases remarkably in comparison with that of the 1st flow curve.

(2) The value of b gradually decreases with increasing number of repetition of loading.

(3) The strain during recovery decreases in direct proportion to the logarithm of time and the tangent of the slope angle of each line representing the strain and the logarithm of time is constant independent of the number of repetitional removal of load.

Above features can be explained theoretically as follows. The flow equation for repetitional loading test should have different relation from Eq. (3.1), because the flow due to the exchange of positions between a particle and its neighbouring hole only takes place at the stress larger than $(\sigma-\sigma_0-\varepsilon_r E_2)$, where ε_r denotes a residual strain at the beginning of the loading.

Then refering to Eq. (3.1), the strain rate $d\varepsilon_2/dt$ is given as follows.

$$\frac{d\varepsilon_2}{dt}=A_2(\sigma-\sigma_0-\varepsilon_r E_2)\sinh\left(\frac{B_2\sigma_2}{\sigma-\sigma_0-\varepsilon_r E_2}\right)$$

$$=A_2(\sigma-\sigma_0-\varepsilon_r E_2)\sinh\left\{\frac{B_2(\sigma-\sigma_0-\varepsilon_2 E_2)}{(\sigma-\sigma_0-\varepsilon_r E_2)}\right\} \qquad (9.1)$$

and refering to Eq. (3.5)

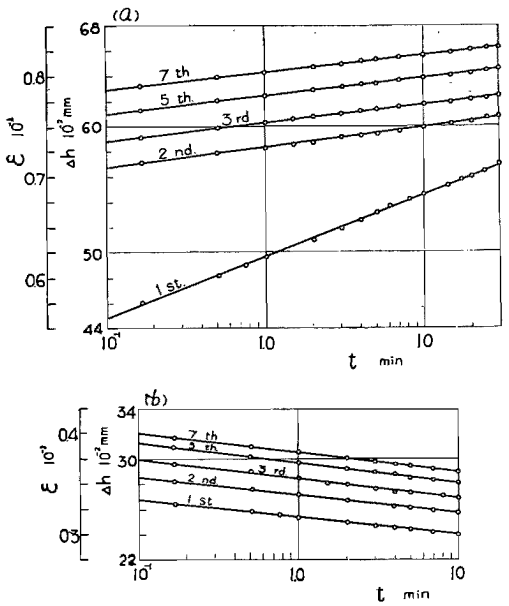

Fig. 2.14 Flow and recovery curves due to repetitional loading (sample ; No. 11, water content ; 71%, $\sigma=0.319$ kg/cm^2, $\sigma_u=0.38$ kg/cm^2, loading time ; 30 min, interval of removal of loading ; 10 min.)
(a) Flow strain vs. time curves
(b) Flow recovery strain vs. time curves

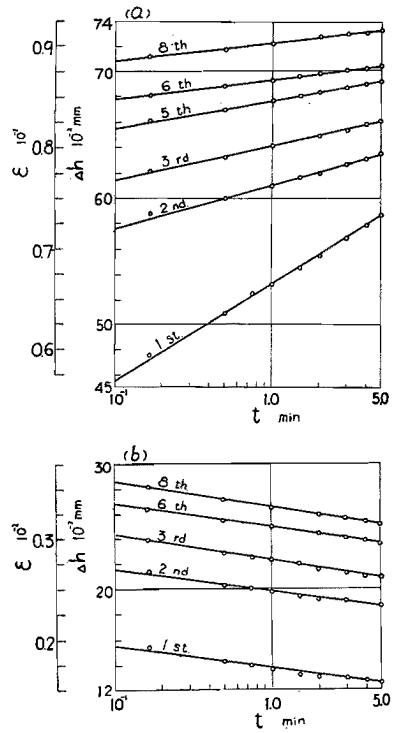

Fig 2.15 Flow and recovery curves due to repetitional loading (sample ; No. 9, water content; 74%, $\sigma=0.218$ kg/cm^2, $\sigma_u=0.34$kg/cm^2. loading time ; 5 min, interval of removal of loading; 5 min)
(a) Flow strain vs. time curves
(b) Flow recovery strain vs. time curves

$$\sigma=\varepsilon_2 E_2+\frac{(\sigma-\sigma_0-\varepsilon_r E_0)}{B_2}\sinh^{-1}\left\{\frac{1}{A_2(\sigma-\sigma_0-\varepsilon_r E_2)}\frac{d\varepsilon_2}{dt}\right\}+\sigma_0 \qquad (9.2)$$

Integrating Eq. (9.1), we obtain

$$\int\frac{d\varepsilon_2}{\sinh\left\{\frac{B_2(\sigma-\sigma_0-\varepsilon_2 E_2)}{(\sigma-\sigma_0-\varepsilon_r E_2)}\right\}}=A_2(\sigma-\sigma_0-\varepsilon_r E_2)\int dt+C$$

from which

$$-\frac{(\sigma-\sigma_0-\varepsilon_r E_2)}{B_2 E_2}\log\tanh\left\{\frac{B_2(\sigma-\sigma_0-\varepsilon_2 E_2)}{2(\sigma-\sigma_0-\varepsilon_r E_2)}\right\}=A_2(\sigma-\sigma_0-\varepsilon_r E_2)t+C \qquad (9.3)$$

The arbitrary constant C is equal to $-\frac{(\sigma-\sigma_0-\varepsilon_r E_2)}{B_2 E_2}\log\tanh\left(\frac{B_2}{2}\right)$, since we have $\varepsilon_2=\varepsilon_r$ at $t=0$.

Substituting this constant into Eq. (9.3), we obtain

$$\log\tanh\left\{\frac{B_2(\sigma-\sigma_0-\varepsilon_2E_2)}{2(\sigma-\sigma_0-\varepsilon_rE_2)}\right\}=-A_2B_2E_2t+\log\tanh\left(\frac{B_2}{2}\right) \tag{9.4}$$

From Eq. (9.4) we get the relation between ε_2 and t.

$$\varepsilon_2=\frac{(\sigma-\sigma_0)}{E_2}-\frac{2(\sigma-\sigma_0-\varepsilon_rE_2)}{B_2E_2}\tanh^{-1}\left\{\exp(-A_2B_2E_2t)\tanh\left(\frac{B_2}{2}\right)\right\} \tag{9.5}$$

If $B_2/2>1$ and

$$2B_2>\frac{2B_2(\sigma-\sigma_0-\varepsilon_2E_2)}{(\sigma-\sigma_0-\varepsilon_rE_2)}>1$$

or

$$\varepsilon_r<\varepsilon_2<\frac{(\sigma-\sigma_0)}{2B_2E_2}(2B_2-1)+\frac{\varepsilon_r}{2B_2} \tag{9.6}$$

Eq. (9.5) is given approximately as

$$\varepsilon_2=\frac{(\sigma-\sigma_0)}{E_2}+\frac{(\sigma-\sigma_0-\varepsilon_rE_2)}{B_2E_2}\log A_2'B_2E_2t \tag{9.7}$$

where $A_2'=A_2/2$.

Substituting Eq. (9.7) into Eq. (3.3), we obtain

$$\varepsilon=\frac{\sigma}{E_1}+\frac{(\sigma-\sigma_0)}{E_2}+\frac{(\sigma-\sigma_0-\varepsilon_rE_2)}{B_2E_2}\log A_2'B_2E_2+\frac{(\sigma-\sigma_0-\varepsilon_rE_2)}{B_2E_2}\log t \tag{9.8}$$

The tangent of the slope angle of the straight lines representing $\varepsilon\sim\log_{10}t$ relations for repetitional loading test is expressed by

$$b=\frac{2.3(\sigma-\sigma_0-\varepsilon_rE_2)}{B_2E_2}=c-d\cdot\varepsilon_r \tag{9.9}$$

where $c=2.3(\sigma-\sigma_0)/B_2E_2$ and $d=2.3/B_2$ are constants.

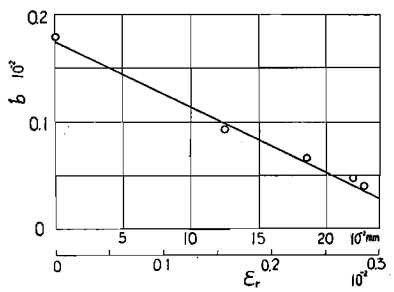

Fig. 2.16 A relation between the coefficient b and residual strain ε_r obtained from Fig. 2.15 (sample No. 9)

As ε_r increases with the number of repetition of loading, Eq. (9.9) indicate that the value of b decreases with increasing number of repetition of loading. This gives rize to the suggestion that the strain-hardening effect and increase of apparent elastic modulus by deformation of clay can be explained from the micrometric standpoint.

An experimental reality of Eq. (9.9) can be showed by Fig. 2.16 which obtained from Fig. 2.15 and illustrates

the linear relationship between b and ε_r. Since this linear relation gives

$$b = c - d \cdot \varepsilon_r$$
$$= 0.00175 - 0.50 \cdot \varepsilon_r,$$

the calculated values of E_2 and B_2 are as follows : $E_2 = 56.5$ kg/cm^2, $B_2 = 4.6$ (In this case, $\sigma = 0.218$ kg/cm^2, $\sigma_0 = 0.02$ kg/cm^2).

Besides, if ε_2 is beyond the limits of (9.6), viz.

$$\varepsilon_2 > \frac{(\sigma - \sigma_0)}{2B_2E_2}(2B_2 - 1) + \frac{\varepsilon_r}{2B_2} \qquad (9.10)$$

Eq. (9.5) becomes

$$\varepsilon_2 = \frac{(\sigma - \sigma_0)}{E_2} \qquad (9.11)$$

at $t \to \infty$.

Substituting Eq. (9.11) into Eq. (3.3), we obtain

$$\varepsilon_{t\to\infty} = \frac{\sigma}{E_2} + \frac{(\sigma - \sigma_0)}{E_2} \qquad (9.12)$$

According to the theory proposed by the authors, therefore, the strain$\sim$log$t$ curve should approach to a horizontal asymptote represented by Eq. (9.12).

Above mentioned results were obtained by experiments performed at the stresses lower than the upper yield value. In order to give a further illustration on rheological behaviour of clay, repetitional flow curves obtained by the experiment performed at a stress larger than the upper yield value are shown in Fig. 2.17 (a). Curves shown in Fig. 2.17 (a) are flow curves obtained by repetitional loading with a stress of $\sigma = 0.436$ kg/cm^2, larger than the upper yield value of $\sigma_u = 0.34$ kg/cm^2, and it is found that all curves rise concave upwards on the semi-logarithmic paper and failure occurs on the way of 4th flowing. It deserves attention that, as above facts indicate, the effect of

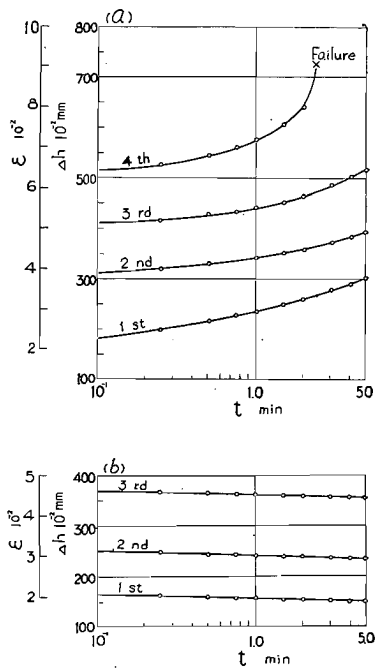

Fig. 2.17 Flow and recovery curves due to repetitional loading (sample No. 9. $\sigma = 0.436$ kg/cm^2, $\sigma_u = 0.34$ kg/cm^2, loading time ; 5 min, interval of removal of loading ; 5 min)
(a) Flow strain vs. time curves
(b) Flow recovery strain vs. time curves

repetitional loading on clay may be harmful if the applied stress is larger than the upper yield value.

In spite of non-linear character of the flow curve due to the repetitional stress larger than σ_u, each flow curve due to recovery after the removal of such stress holds linear character, and the each slope of the flow recovery curve is nearly equal as shown in Fig. 2.17(b).

The theoretical analysis of the flow recovery is as follows. Since the restraining stress σ_0 acts in the opposite direction to the recovering stress $\varepsilon_2 E_2$ after removal of the stress, we put $\sigma_0 = -\sigma_0$ and $\sigma = 0$ in Eq. (3.5). And ε_1 in Eq. (3.3) is equal to zero in this case, because the total recovering deformation of the spring element E_1 shown in. Fig. 1.3 takes place immediately after removal of the load. Therefore, we get the following equation.

$$\varepsilon E_2 - \sigma_0 + \frac{\sigma_0}{E_2} \sinh^{-1}\left(\frac{1}{A_2\sigma_0}\frac{d\varepsilon}{dt}\right) = 0 \tag{9.13}$$

Transformation of Eq. (9.13), leads to;

$$\frac{d\varepsilon}{dt} = -A_2\sigma_0 \sinh\left\{\frac{B_2}{\sigma_0}(\varepsilon E_2 - \sigma_0)\right\} \tag{9.14}$$

from which

$$\frac{\sigma_0}{B_2E_2} \log\tanh\left\{\frac{B_2}{2\sigma_0}(\varepsilon E_2 - \sigma_0)\right\} = -A_2\sigma_0 t + C \tag{9.15}$$

Since we have the residual deformation ε_a at the beginning of the flow recovery, the arbitrary constant C is decided to $\frac{\sigma_0}{B_2E_2} \log\tanh\left\{\frac{B_2}{2\sigma_0}(\varepsilon_a E_2 - \sigma_0)\right\}$ by putting $\varepsilon = \varepsilon_a$ and $t = 0$ in Eq. (9.15).

Substituting this constant into Eq. (9.15), we obtain

$$\log\tanh\left\{\frac{B_2}{2\sigma_0}(\varepsilon E_2 - \sigma_0)\right\} = -A_2B_2E_2t + \log\tanh\left\{\frac{B_2}{2\sigma_0}(\varepsilon_a E_2 - \sigma_0)\right\} \tag{9.16}$$

From Eq. (9.16) we get the relation between ε and t.

$$\varepsilon = \frac{\sigma_0}{E_2} + \frac{2\sigma_0}{B_2E_2}\tanh^{-1}\left[\exp(-A_2B_2E_2t)\tanh\left\{\frac{B_2}{2\sigma_0}(\varepsilon_a E_2 - \sigma_0)\right\}\right] \tag{9.17}$$

So far as

$$\varepsilon_a > \varepsilon > \frac{\sigma_0}{2B_2E_2}(1 + 2B_2) \tag{9.18}$$

The following approximate result is given as

$$\varepsilon = \frac{\sigma_0}{E_2} - \frac{\sigma_0}{B_2E_2}\log A_2' B_2E_2 - \frac{\sigma_0}{B_2E_2}\log t \tag{9.19}$$

where $A_2' = A_2/2$.

If ε is beyond the limits of (9. 18), viz.

$$\varepsilon < \frac{\sigma_0}{2B_2E_2}(1+2B_2) \tag{9.20}$$

Eq. (9. 17) becomes

$$\varepsilon_{t\to\infty} = \frac{\sigma_0}{E_2} \tag{9.21}$$

at $t\to\infty$.

Eq. (9. 19) and Eq. (9. 21) indicate that the strain$\sim$log$t$ relation of flow recovery is linear and the slope of the line, viz. the value of σ_0/B_2E_2, is constant independent of residual strain ε_a, and moreover the strain$\sim$log$t$ curve should approach to a horizontal asymptote represented by Eq. (9. 21).

10 Summary

In this chapter, various experiments and their considerations of compression flow are carried out on undisturbed clay, in order to refer and ascertain the theory derived in Article 3. On the basis of the theory and experiments on rheological properties of undisturbed clay reported in this paper, the following conclusions are believed to be warranted so far as the applied stress σ is less than the pre-consolidation stress and the upper yield value σ_u of the clay.

(1) The results of the compression flow tests on undisturbed clay well agree with the theory stated in Article 3 in which the authors proposed the existence of restraining resistance σ_0 which prevents the displacement of particle to neighbouring hole, and the new structural viscosity obtained by the assumption that the number of the unit processes of deformation N_t or n_t are directly proportional to stress $(\sigma-\sigma_0)$ when the applied stress is less than the upper yield value σ_u and the pre-consolidation stress of the clay.

The details of (1) are summarized in the following articles.

(2) Taking flow strain as ordinate in ordinal scale and loading time as abscissa in logarithmic scale, this relation is expressed by straight line, and the tangent of slope angle of this straight line increases linearly with applied stress (c.f. Fig. 2. 4, 2. 5, 2. 6).

(3) If the stress larger than the upper yield value is applied, the flow strain increases acceleratively and failure takes place after a certain duration (c.f. Fig. 2.4, 2.5, 2.6).

Only in this case, theory stated in (1) does not hold.

(4) The linear relation between strain rate of flow and loading time holds if they are plotted on the logarithmic paper, and the slope of the straight line is constant independent of applied stress (c.f. Fig. 2. 9, 2. 10).

(5) There holds also linear relation between strain rate of flow and applied stress for various constant values of loading time (c.f. Fig. 2. 8).

(6) It is presumed that the rate of strain increases with increasing values of temperature at constant water content.

(7) The relation between the flow strain at a certain elapsed time and the applied stress are linear and the authors analysed the character of the time-function $\phi(t)$ (c.f. Fig. 2. 11, 2. 12).

(8) Taking flow strain as ordinate in ordinal scale and loading time as abscissa in logarithmic scale for repetitional loading test, the relation is expressed by straight line. The tangent of slope angle of this straight line decreases direct proportionally to the residual strain ε_r which rests at the biginning of the loading and increases with the number of repetition of loading (c.f. Fig. 2. 16).

(9) The strain during flow recovery decreases in direct proportion to the logarithm of time and the tangent of the slope angle of each line representing the strain and the logarithm of time is constant independent of the number of repetitional removal of load (c.f. Fig. 2. 14 (b), 2. 15 (b)).

Chapter 3 Long-term Strength

11. Aim and Brief Contents

The investigations on the long-term strength or the stress expressed at flow failure are important for the problems on the critical bearing capacity of foundation, the stability of slope or the analysis of land-slide. As the long-term strength has close connection with the upper yield value mentioned in the preceding chapter, a new measuring method of the yield value founded on the preceding theory is proposed and a new formula relating between long-term strength and the time lapse necessary to flow failure is derived. Researching experimentally on the relations between the upper yield value, strengths by the stress- or strain-controlled tests and the water content with undisturbed clay samples of various water contents, new important results have been obtained. In addition, the effect of flow on the strength of clay

is experimented and considered.

The clay samples and the testing apparatus used on the experiments related in this chapter are the same with those described in Article 5. Therefore the sample number denoted in this chapter can be refered to the soil profile shown in Fig. 2. 1.

12. A Method to Measure the Upper Yield Value of Clay by Stress-controlled Compression Test

If a stress exceeding the upper yield value is applied on clay, the clay fails after increasing its flowing speed. Though the upper yield value can be determined graphically with the viscosity curve obtained by means of the compression flow tests as stated in Article 7, such determining procedure is troublesome and requires much time and much fresh specimens made of the same sample.

As an improved method to measure the upper yield value of clay, instead of the above stated complex procedure, the authors propose a new method using the so-called stress-controlled compression test which can be performed simply and quickly with the common type of load-controlled compression apparatus. In this case, load-controlled test is considered to be stress-controlled test if the slight change in sectional area caused by lateral expansion is neglected. On this test, the compressive stress is applied by equal stress increment at uniform time interval stepwise as shown in Fig. 3. 1 and compressive strain is measured at each end of the step of stress. The ratio of stress increment σ_c and time interval t_c is defined as the rate of stress-increment α, therefore $\alpha=\sigma_c/t_c$.

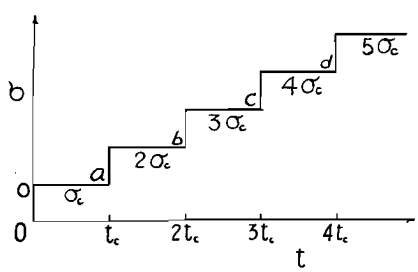

Fig. 3.1 Schematic relation of stress vs. time in stress-controlled compression process to determine the upper yield value

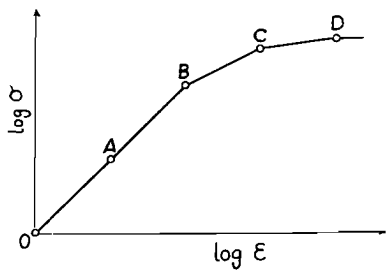

Fig. 3.2 Logarithmic relation of stress vs. strain in stress-controlled compression process to determine the upper yield value

A stress~strain relation obtained by a stress-controlled test with an α on an undisturbed clay sample can be illustrated as a broken line $OABCD$ as shown in Fig. 3. 2 on the logarithmic paper. In Fig. 3. 2 points O, A, B, C, D.....correspond to the points o, a, b, c, d.....in Fig. 3.1 and first few points e.g. O, A, B lie on the same straight line, therefore point B becomes a first inflection point.

The linearity of the line OB can be explained theoretically as follows. In the case of stress-controlled test, we have to consider the effect of the residual strain ε_r as stated in Article 9, because the process of stress-controlled test is considered to be analogus with the repetitional loading test with successively applied loads of σ_c, $2\sigma_c$, $3\sigma_c$,...and $n\sigma_c$. In Eq. (9. 7) representing the strain~time relation of modified Voigt element for repetitional loading test, the lower yield value σ_0 is considered negligibly small compared with the applied stress σ, therefore the strains of modified Voigt element $\varepsilon_{2.1}$, $\varepsilon_{2.2}$, $\varepsilon_{2.3}$,....and $\varepsilon_{2.n}$ can be expressed as follows. Where the 1st suffix 2 of $\varepsilon_{2.i}$ expresses the strain of modified Voigt element at the end of each loading step and the 2nd suffix i of $\varepsilon_{2.i}$ the number of loading step.

$$\varepsilon_{2.1}=\frac{\sigma_c}{E_2}(1+l)\equiv\varepsilon_{r.1}$$

$$\varepsilon_{2.2}=\frac{2\sigma_c}{E_2}(1+l)-l\varepsilon_{r.1}=\varepsilon_{r.1}(2-l)\equiv\varepsilon_{r.2}$$

$$\varepsilon_{2.3}=\frac{3\sigma_c}{E_2}(1+l)-l\varepsilon_{r.2}=\varepsilon_{r.1}(3-2l+l^2)\equiv\varepsilon_{r.3}$$

$$\cdots\cdots\cdots\cdots\cdots\cdots\cdots\cdots\cdots\cdots$$

$$\begin{aligned}\varepsilon_{2.n}&=\varepsilon_{r.1}\{n+(n-1)(-l)+(n-2)(-l)^2+\cdots\cdots\\&\quad+2(-l)^{n-2}+(-l)^{n-1}\}\\&=\frac{\sigma_c}{E_2}[n-\{(-l)+(-l)^2+(-l)^3+\cdots\cdots+(-l)^n\}]\end{aligned}\tag{12. 1}$$

where $l=\frac{1}{B_2}\log A_2'B_2E_2t_c$, and $-1<l<0$ because $0<\frac{\sigma}{E_2}\left(1+\frac{1}{B_2}\log A_2'B_2E_2t\right)$ $<\frac{\sigma}{E_2}$, $\varepsilon_{r.1}$, $\varepsilon_{r.2}$, $\varepsilon_{r.3}$·····and $\varepsilon_{r.n}$ denote residual strains at the ends of the loading steps of 1, 2, 3·····n respectively.

Then the total strain at the end of the nth loading step ε_n is given by

$$\begin{aligned}\varepsilon_n&=\varepsilon_{1.n}+\varepsilon_{2.n}\\&=\frac{n\sigma_c}{E_1}+\frac{n\sigma_c}{E_2}-\frac{\sigma_c}{E_2}\{(-l)+(-l)^2+(-l)^3+\cdots\cdots+(-l)^n\}\end{aligned}\tag{12. 2}$$

where $\varepsilon_{1.n}$ is the strain of a spring element E_1.
Eq. (12. 2) represents the stress ($\sigma = n\sigma_c$)~strain relation for stress-controlled compression test.

The results of the stress~strain relations numerically calculated by Eq. (12. 2) are shown in Fig. 3. 3 for various values of l and these calculated curves are represented by approximate straight lines on the logarithmic paper. In these calculations the values of constant terms in Eq. (12. 2) are founded on the experiments of Fig. 2. 15 (in the case of clay sample No. 9) as follows. The first elastic modulus E_1 ($=393 kg/cm^2$) was obtained as the ratio of the stress $\sigma = 0.218 kg/cm^2$ to the instantaneous strain $\varepsilon_1 = 5.55 \times 10^{-4}$ Comparative calculation of E_1 showed so excellent agreement as the value above obtained is equal to the instantaneous modulus of recovering deformation ($E_1 = 392 kg/cm^2$) computed from the flow recovery curve shown in Fig. 2. 15 (b). The second elastic modulus E_2 was equal to $56.5 kg/cm^2$ as stated in Article 9. The stress increment σ_c is $0.1 kg/cm^2$. The calculated values of Eq. (12. 2) against $l = -1/2$, $-1/10$, and $-1/100$ are shown in Fig. 3. 3 and the slope angle of line β increases with increasing the value of l. It is obvious that the upper limit value of β is given when $l = 0$ and is equal to 45°.

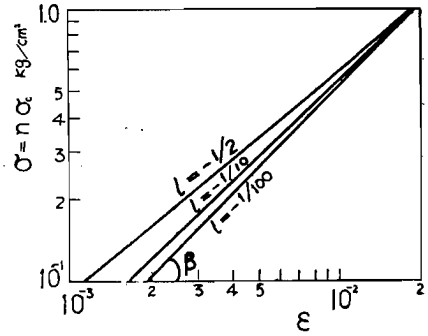

Fig. 3.3 Results of numerical calculations of Eq. (12.2)

As Eq. (9. 7) holds only for the stress below the upper yield value, Eq. (12. 2) holds also within this stress region and the stress at the first inflection point from which Eq. (12. 2) does not hold should correspond to the upper yield value. Therefore the upper yield values of clay can be measured as the stress corresponding to the first inflection point of stress~strain curve on logarithmic paper obtained by the stress-controlled unconfined compression test, which is performed by adding equal stress increment at uniform time interval.

Fig. 3. 4 gives an example of logarithmic relations between stress and strain obtained with three clay samples applying the rate of stress increment of $\alpha = 5 \times 10^{-3} kg/cm^2/min$. From the experimental curves in Fig. 3. 4, stresses corresponding to the points of first inflection of curves are obtained as shown in center column of Table 3. 1. Each stress tabulated in the center column

Table 3.1

Sample No.	Stress corresponding to the point of first inflection of curve kg/cm²	Upper yield value kg/cm²
13	0.44	0.45
8	0.34	0.33
4	0.19	0.19

well agrees with the each value tabulated in the right column of Table 3. 1 respectively which is the upper yield value obtained by the graphical procedure in Fig. 2. 8 and tabulated in Table 2. 1.

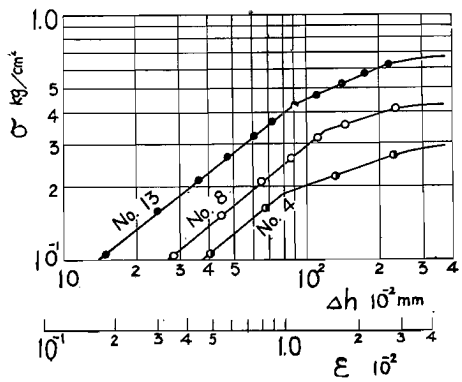

Fig. 3.4 Logarithmic relations between the applied stress σ and strain ε

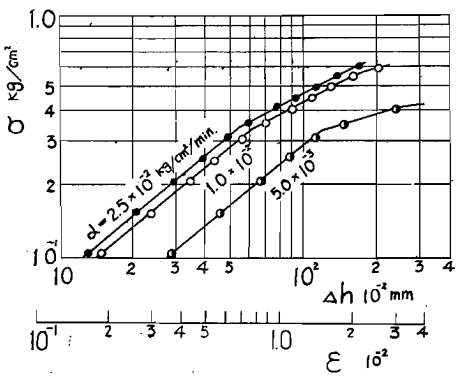

Fig. 3.5 Logarithmic relations between the applied stress σ and strain ε at various rates of stress-increment (sample No. 8)

According to the above mentioned theoretical consideration and actual proof with experimental results, it becomes possible to obtain the upper yield value by means of the unconfined stress-controlled compression test.

Besides undisturbed clay, it was observed experimentally that concrete[9] and some kinds of metal have the same flow character as mentioned above: that is, stress~strain relations of such materials represented on logarithmic paper were straight lines continuing to the upper yield stresses.

It is a well known fact that the so-called stress~strain curve and the failure strength obtained by the ordinary compression test are influenced to a certain extent by either the rate of deformation or the rate of stress-increment and the failure strength increases with the rate of stress-increment. On the other hand, as shown in Fig. 3. 5, the effect of the rate of stress-increment on the upper yield value is negligible; that is, the each stress corresponding to the

point of first inflection of the curve obtained by the each stress-controlled test of different rate of stress-increment ($\alpha=5\times10^{-3}$, 1×10^{-2} or 2.5×10^{-2} kg/cm^2 /min) on the same clay (sample number of clay: No. 8) is nearly equal to 0.33 kg/cm^2

Next, a series of stress-controlled undrained triaxial compression tests at $\alpha=5\times10^{-3}$kg/cm^2/min was performed with undisturbed saturated clay of 70% water content (sample number of clay: No. 17) to fined the failure strength and the upper yield value. In these tests, applied compressive stresses were restrained not exceed the pre-consolidation pressure of the clay. Fig. 3.6 shows

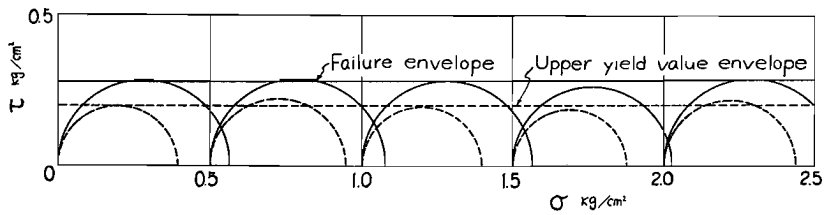

Fig. 3.6 Envelopes of both failure and upper yield value by stress-controlled Q-test (samle No 17)

the Mohr's circles and their envelopes for the five tests in which no consolidations either before or during compression tests are permitted. Each circle for the upper yield value in Fig. 3. 6 is drawn with the ambient pressure and the stress at the point of first inflection of the stress~strain curve obtained by the same procedure as that of the unconfined stress-controlled compression test. Since the ambient pressure is carried by the pore water on the undrained triaxial test and, accordingly, generates no additional strength in clay, both the envelope of circles of ruptures and that of the upper yield values σ_u are horizontal inspite of intensity of the ambient pressure. In Fig. 3. 6, deviator stresses for rupture and upper yield value are measured as 0.55 kg/cm^2 and 0.40 kg/cm^2 respectively.

As the fact that the upper yield value does not be influenced by the ambient pressure of triaxial stress-controlled compression test means that rheological constants (A_2, B_2) of clay in Eq. (12. 2) also indifferent from the ambient pressure, it may be concluded that the strain rate of clay does not be influenced by the ambient pressure. This conclusion had been observed experimentally by R.Haefeli[5] with undrained triaxial compression test.

13. Effect of Water Content on the Upper Yield Value and on the Compressive Strength

In order to research the effect of water content on the upper yield value of undisturbed saturated clay, a large number of stress-controlled unconfined compression test introduced in preceding article has been performed on undisturbed saturated clay of same kind but with various water contents. In addition to these tests, using the same kind of undisturbed saturated clay with various water contents their failure strengths were measured by two kinds of unconfined compression tests;—one is the strain-controlled test whose strain speed is 1% of the original height of the specimen per minute and the other is the stress-controlled test whose rate of stress increment α is 5×10^{-3} kg/cm^2 per minute.

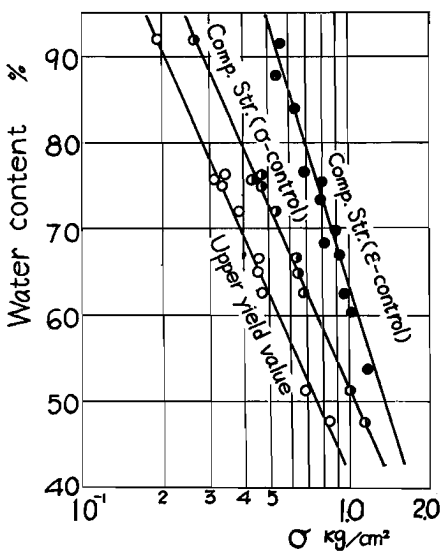

Fig. 3.7 Relations between water content and strengths (upper yield value, compressive strengths by stress-controlled and strain-controlled test)

Results of these tests are shown in Fig. 3. 7. From this figure the following matters may be concluded.

(1) If the unconfined compressive strengths measured by the strain-controlled test and the stress-cnotrolled test and the upper yield values of undisturbed saturated clay are plotted against their water contents on a semi-logarithmic paper as shown in Fig. 3. 7, it is clear that the linear relations hold for each kinds of strength and the upper yield value within a range of permissible error.

Among these relations, relations between water content w and compressive strength by the strain-controlled test σ_n have been reported to be represented by following equation as a result of a theoretical consideration[10].

$$\sigma_n=\bar{A}_n\exp\left(-2.3\frac{w}{\bar{B}_n}\right) \qquad (13.\ 1)$$

where $\bar{A}_n$, $\bar{B}_n$; constants.

If the same form of equation is applied for the compressive strength by the stress-controlled test σ_s and the upper yield value σ_u, relations between water content w and σ_s or σ_u as shown in Fig. 3. 7 can be represented as follows;

$$\left.\begin{aligned}\sigma_s &= \bar{A}_s \exp\left(-2.3\frac{w}{\bar{B}_s}\right)\\ \sigma_u &= \bar{A}_u \exp\left(-2.3\frac{w}{\bar{B}_u}\right)\end{aligned}\right\} \qquad (13.\ 2)$$

where $\bar{A}_s$, $\bar{B}_s$, $\bar{A}_u$, $\bar{B}_u$; constants.

(2) As the left line and center one in Fig. 3. 7 are parallel each other, the ratio of the upper yield value and the failure strength obtained by the stress-controlled compression test is constant at the same water content and this ratio is nearly equal to 0.71, independent of water content of clay.

From this result, following relations hold among the constants of Eq. (13. 2).

$$\bar{B}_s = \bar{B}_u \qquad (13.\ 3)$$

then

$$\frac{\sigma_u}{\sigma_s} = \frac{\bar{A}_u}{\bar{A}_s} = 0.71 \qquad (13.\ 4)$$

(3) The ratio of the upper yield value and the failure strength obtained by the strain-controlled test (σ_u/σ_n) is not constant but increases with decreasing of water content. This ratio varies from 0.36 to 0.57 according as water content decreases from 90 to 50% for the clay tested here.

Results obtained in this article are important and very useful for the practical investigation such as the calculation of stability of slope or bearing capacity of foundation which support almost constant load. As the upper yield value of clay is smaller than its strength measured by the strain-controlled or stress-controlled tests, the calculated critical strength of soil structure or foundation which is based on the failure strength of clay obtained by the ordinary strain-controlled testing method lies in dangerous side as compared with true critical strength (or upper yield value) below which the load is supported permanently.

14. Long-term Strength

As already stated, if any constant stress exceeding the upper yield value is applied on clay, the clay fails after it flows. Since the authors defined such

stress as exceeds the upper yield value the long-term strength, the long-term strength does not mean a definite value.

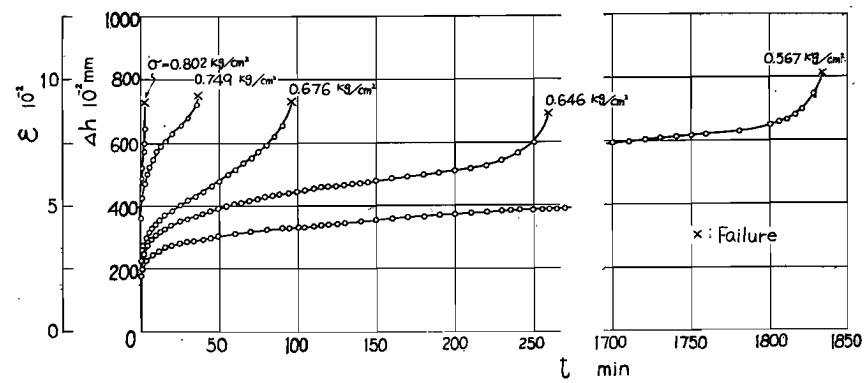

Fig. 3.8 Characteristic curves of the flow failure under various stresses

Fig. 3.8 illustrates the flow curves and points where failures took place obtained by the unconfined compression tests under various constant stresses σ exceeding the upper yield value on undisturbed clay specimens made from sample No. 13. The general feature of such a flow curve consists of three main stages of deformation ; that is, a stage of flow at a decelerating rate which appears a while after the application of compression, next to this stage, a stage at an approximately constant rate and finally a stage at an accelerating rate leading to failure. As this feature is quite different from that of the flow at the stress below the upper yield value, the mechanism of flow at the stress exceeding the upper yield value must differ from that stated in Article 3.

Moreover, in Fig. 3. 8 it is observed that every flow strain value at failure is almost same irrespective of the intensity of applied stress[11], but the higher the intensity of the long-term strength, the shorter the elapsed time until the flow failure.

About the relation between the long-term strength and the elapsed time to failure the authors solved as follows, applying the theory deduced from the statistical mechanics on the structure of clay.

In the Articles 6 and 9, it was clarified that, when the stress exceeding the upper yield value was applied on clay, the rate of flow strain showed the marked increase and acceleration as compared with the rate of flow strain at the stress lower than the upper yield value. This fact is considered to be caused by the successive breaking of bond between clay particles, which

is caused by the application of external stress exceeding the upper yield value and leads to flow failure after a certain duration. Therefore, if the number of such bonds per unit cross sectional area perpendicular to the direction of the applied stress of clay is N_b, the failure takes place when the number of remaining bonds become zero (when $N_b=0$).

Since the ratio of number of activating bonds per unit time (dN_b/dt) and total bonds (N_b) is equal to the probability or the frequency of activation of one bond per unit time, if repair of broken bonds are prospective, the rate of breaking of such bonds at constant stress σ is written as follows ;

$$-\frac{1}{N_b}\frac{dN_b}{dt}=\frac{2\kappa T}{h}\exp\left(\frac{-E_0}{\kappa T}\right)\sinh\left(\frac{\lambda\sigma_2}{2N_b\kappa T}\right) \tag{14. 1}$$

where κ, h, λ and E_0 are the same notations as denoted in Article 2, σ_2 is the stress applied on the dashpot shown in Fig. 1. 3, and

$$\sigma_2=(\sigma-\sigma_0)-\varepsilon_2 E_2$$

At the state near failure, elastic property of clay become unconspicuous with decreasing the value of N_b and the lower yield value σ_0 is negligibly small compared with the applied stress σ, hence σ_2 is,

$$\sigma_2\fallingdotseq(\sigma-\sigma_0)\fallingdotseq\sigma=\text{const.} \tag{14. 2}$$

Therefore Eq. (14. 1) becomes

$$-\frac{1}{N_b}\frac{dN_b}{dt}=\frac{2\kappa T}{h}\exp\left(\frac{-E_0}{\kappa T}\right)\sinh\left(\frac{\lambda\sigma}{2N_b\kappa T}\right) \tag{14. 3}$$

When the intensity of applied stress σ is high or the repair of the bonds does not expecting, the equation is

$$-\frac{1}{N_b}\frac{dN_b}{dt}=\frac{\kappa T}{h}\exp\left(\frac{-E_0}{\kappa T}\right)\exp\left(\frac{\lambda\sigma}{2N_b\kappa T}\right) \tag{14. 4}$$

By the substitution $u=\sigma/BN_b$, we obtain the following :

$$\int_{u_0}^{\infty}\frac{1}{u}\exp(-u)du=At_f \tag{14. 5}$$

where

$$A=\frac{\kappa T}{h}\exp\left(\frac{-E_0}{\kappa T}\right),\qquad B=\frac{2\kappa T}{\lambda},\qquad u_0=\frac{\sigma}{BN_{bo}}$$

and t_f is the time lapse necessary to the flow failure, N_{bo} the initial number of bonds per unit area of clay.

The upper limit of the integral in Eq. (14. 5) is infinite because when

the clay fails the number of remaining bonds is zero.

The integral $\int\frac{1}{u}\exp(-u)du$ is the well-known logarithmic integral expressed as $-E_i(-u)$, and the table of $E_i(u)$ is published and applicable for the calculation. But for sufficiently large value of u,

$$-E_i(-u)\fallingdotseq\frac{1}{u}\exp(-u) \tag{14. 6}$$

Therefore Eq. (14. 5) becomes approximately

$$\frac{BN_{b0}}{\sigma}\exp\left(\frac{-\sigma}{BN_{b0}}\right)=At_f \tag{14. 7}$$

Taking the logarithm of each term, we get

$$\begin{aligned}\log t_f&=\log\frac{1}{A}-\log\frac{\sigma}{BN_{b0}}-\frac{\sigma}{BN_{b0}}\\&=\log\frac{h}{\kappa T}+\frac{E_0}{\kappa T}-\log\frac{\lambda\sigma}{2N_{b0}\kappa T}-\frac{\lambda\sigma}{2N_{b0}\kappa T}\end{aligned} \tag{14. 8}$$

When the intensity of stress is so high as the 3rd term $\log(\lambda\sigma/2N_{b0}\kappa T)$ of the right hand side in Eq. (14. 8) becomes negligibly small compared with the 4th term $(\lambda\sigma/2N_{b0}\kappa T)$, Eq. (14. 8) can be written approximately by

$$\log t_f=\log\frac{h}{\kappa T}+\frac{E_0}{\kappa T}-\frac{\lambda\sigma}{2N_{b0}\kappa T} \tag{14. 9}$$

or

$$\log_{10}t_f=\log_{10}\frac{h}{\kappa T}+\frac{E_0}{2.3\kappa T}-\frac{\lambda\sigma}{4.6N_{b0}\kappa T} \tag{14. 10}$$

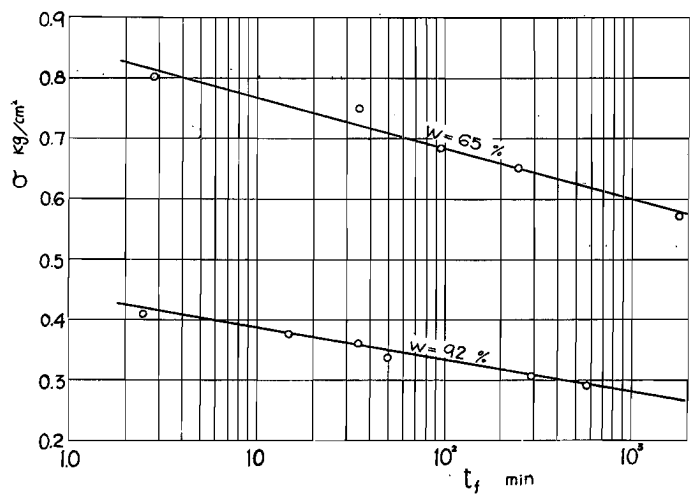

Fig. 3.9 Relations between the long-term strength and the time to failure (sample No. 13, water content ; 65%, sample No. 2～5, water content ; 92%)

The results of some tests for the flow failure are given in Fig. 3. 9 which shows the relations of $\sigma \sim \log t_f$ obtained for the clay samples of No. 13 (water content=65%) and No. 2~5 (water content=92 %). Since the experimental data lie in well agreement on straight lines on a semi-logarithmic scale, it can be said that the each relation between the long-term strength of clay and the time to failure is quite satisfactorily expressed by Eq. (14. 10), and the tangent of the slope angle of each line is equal to the values of $\lambda/4.6N_{b0}\kappa T$.

If $\log_{10} t_f$ at $\sigma=0$ is written as $\log_{10} t_{f.i}$, the actual value of $\log_{10} t_{f.i}$ is obtained by the abscissa of the point where the axis of $\sigma=0$ and extrapolating the line in Fig. 3. 9 experimentally obtained intersects. As the equation of $\log_{10} t_{f.i}$ is given by

$$\log_{10} t_{f.i} = \log_{10} \frac{h}{\kappa T} + \frac{E_0}{2.3\kappa T} \qquad (14.\ 11)$$

the value of E_0 can be computed from Eq. (14. 11). Curves of $\sigma \sim \log t_f$ shown in Fig. 3. 9 are given for clay samples of No. 13 and No. 2~5.

Clay No. 13 ; $\sigma = 0.845 - 0.084 \log_{10} t_f$

Clay No. 2~5 ; $\sigma = 0.437 - 0.053 \log_{10} t_f$

therefore, by putting $\sigma=0$ we obtain $\log_{10} t_{f.i}$ as follows

Clay No. 13 ; $\log_{10} t_{f.i} = 10.07$

Clay No. 2~5 ; $\log_{10} t_{f.i} = 8.24$

On the other hand, as $\log_{10} t_{f.i}$ is represented by Eq. (14. 11) and temperature during the experiment was 10°C (or absolute temperature $T=273.2+10=283.2$°K), the values of activating free energy E_0 can be computed by substituting the values in Table 3. 2 into Eq. (14. 11). The values of E_0 thus calculated are shown in the 5th column of Table 3. 2 and have order of 10^{-12} erg respectively.

Table 3.2

Sapmle No.	Water content %	$t_{f.i}$ min	$h/\kappa T$ min	E_0 erg
13	65	1.18×10^{10}	2.82×10^{-15}	2.21×10^{-12}
2~5	92	1.74×10^{8}	2.82×10^{-15}	2.05×10^{-12}

Note : Planck's const $h=6.626\times10^{-27}$ erg. sec
Boltzman's const $\kappa=1.3808\times10^{-16}$ erg. deg^{-1}

15. Effect of Flow on the Strength of Clay

Some results of this effect above tilted were reported by other researchers.

A. Casagrande and D. Wilson[12] said that this effect is often considerable and it may be either favourable or unfavourable effect on the strength of clay according to the type of soil. R. Haefeli[6] gave the results of two weeks' flow by the triaxial compression test which showed a certain increase of about 20 ~30% in the compressive strength according with the applied shearing stress of intensity of 0.55 kg/cm².

No attention was paid in their reports, however, to the relation of intensity of the applied flow stress and the upper yield value. It may be suggested that the strength of clay will increase after the flow at the stress lower than the upper yield value but will decrease at the stress higher than it, because it is clarified that, from the results of flow tests by repetitional loading as stated in Article 9, the rate of strain by the stress lower than the upper yield value decreases with the number of repetition, on the other hand the rate of strain by the stress higher than it has another behaviour as shown in Fig. 2. 17.

On the basis of the above suggestion, the authors investigated the effect of the flow on the compressive strength of clay when the flow is caused by applying the constant stress lower than the upper yield value. As a series of experiments, constant compressive stress of 0.24 kg/cm² lower than $\sigma_u = 0.36$ kg/cm² was applied on the clay samples of No. 11 and 12 with the several durations of the loading from 1 to 5 days, and the common unconfined compression tests (whose rate of strain is 1% of the height of specimen per minute) were performed after removal of the load. Results of these tests (q_u) are shown in the 2nd column in Table 3. 3. Strengths shown in the 4th column in Table 3. 3 are the estimated compressive strengths of the undisturbed clay which receive no flowing stress yet. These "estimated compressive strengths (q_{ue})" are the strengths of the undisturbed clay of the same sample correspond-

Table 3.3

Duration of application of load (day)	Unconfined compressive strength after flow (q_u kg/cm²)	Water content at the test for q_u (w %)	Estimated compressive strength of undisturbed clay (q_{ue} kg/cm²)	Strength ratio (q_u/q_{ue})
1	0.924	71.0	0.860	1.075
2	1.008	67.6	0.930	1.085
3	1.176	60.0	1.070	1.098
4	0.976	69.4	0.880	1.108
5	1.092	64.2	0.990	1.107

ing to the water contents at the above mentioned tests for q_u by applying the water content~strength line of strain-controlled test at the same strain rate shown in Fig. 3. 7.

The 5th column in Table 3. 3 and Fig. 3.10 show the relation of ratio of strength before and after flow (q_u/q_{ue}) and duration time of the flow. As shown in Fig. 3. 10 the strength of clay after application of the constant stress lower than the upper yield value increases with the duration time of flow.

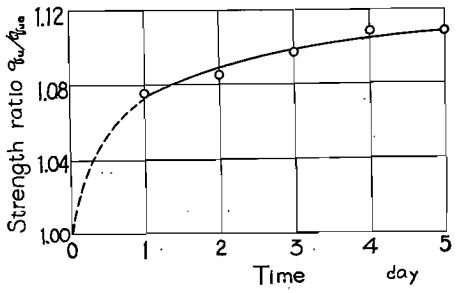

Fig. 3.10 A relation of strength ratio of before and after flow and duration time of the flow

16. Summary

In this article the results of experimental and theoretical studies in this chapter are summarized.

(1) The upper yield values of clay can be measured as the stress corresponding to the first inflection point of stress~strain curve on logarithmic paper obtained by the stress-controlled compression test, which is performed by adding equal stress-increment at uniform time interval.

(2) Though the failure strength is effected by the rate of stress-increment of above mentioned stress-controlled compression test, the upper yield value is almost indifferent from the rate of stress-increment.

(3) The envelope of the Mohr's circles of the upper yield value obtained by undrained triaxial test are horizontal as well as the envelope of failure strength obtained by the same test.

(4) The ratio of the upper yield value and the failure strength obtained by the stress-controlled test is constant and almost equal to 0.71 irrespective of water content of clay.

(5) Eq. (14.9) representing the relation between the long-term strength and the time to failure well agrees with the experimental results.

(6) The strength of clay increases gradually with duration of the flow when a constant stress smaller than the upper yield value is applied on the clay.

Conclusion

In this paper, the rheological characters of clay are researched, and the summaries of the research are as follows (besides, the detailed summary have been already reported in Articles 10 and 16).

In chapter 1, the fundamental character of clay under a constant external stress, that is, the flow character of clay is derived from the micrometric standpoint applying following assumptions. (1) The viscosity of clay exerting on the flow of clay is assumed as the structural viscosity which is derived by applying the statistical mechanics on the frequency of the mutual exchange of position between a clay particle and the neighbouring hole or the point of irregularity in the arrangement of particles. (2) The mechanical model of clay is assumed from the consideration on the structure of clay as the model as shown in Fig. 1.3. (3) The fundamental relation of flow of clay obtained applying above assumption is supposed to be valid so far as the external stress applied on clay is less than either the stress of pre-consolidation or the upper yield value.

Chapter 2 is a report on the experimental results and their considerations of a series of compression flow tests of clay to refer and ascertain the formula derived in Chapter 1. Any flow characters of clay in the experiments—such characters as strain~time, strain-rate, stress~strain expressed by time-function, flow by repetitional loading, flow recovery—exactly agree with the formula so far as the intensity of applied flow stress is less than either the pre-consolidation pressure or the upper yield value.

In Chapter 3, some important problems on soil strength—such as the effect of water content on the failure strength as well as the upper yield value, the relation between the failure strength and the time lapse necessary for failure and the variation in strength by flow—are researched theoretically and experimentally. Then, a new measuring method of the upper yield value of clay is proposed; that is, the upper yield value of clay can be measured as the stress corresponding to the first inflection point of stress~strain curve on logarithmic paper obtained by the stress-controlled compression test performed by adding equal stress increment at uniform time interval.

Furthermore, the values of rheological constants (B_2, E_1, E_2) and activating free energy of clay (E_0) are computed and it is ascertained that these calculated values are of the right order of magnitude.

As the rheological characters of clay are important not only for the problems on the soil mechanics but also for the applications on the practical works, this paper would give some contributions on the soil mechanics and the soil engineering.

Although this paper, subtitled as "Part 1", is only a partial report on the rheological characters of clay under the statical stress less than the pre-consolidation pressure, the authors have arleady researched on the characters of clay on the consolidation and their secondary time effect under the stress larger than the pre-consolidation pressure and on the dynamic behaviours under the vibrating stress, and these above stated researches have reported on some Japanese papers. These results shall be translated in English and published in near future in the Bulletin of this Institute as the supplementary paper.

References :

1) J.M. Burgers and G.W. Scott Blair : Report on the principles of rheological nomenclature, Proc. Ist Int. Congr. Rheol., 1949.
2) A.V. Tobolsky and H. Eyring : Mechanical Properties of Polymeric Materials, J. Chem. Phys., Vol. 11, 1943. pp. 125-134.
3) S. Glasstone, K.J. Laidler and H. Eyring : The Theory of Rate Process, New York, 1941, p. 477.
4) W. Kuhn : Beziehungen zwischen Viscosität und elastischen Eigenschaften amorpher Stoffe, Z. Phys. Chem., B 42, 1939, pp. 1-38.
5) R. Haefeli : Creep Problems in Soils, Snow and Ice, Proc. 3rd Int. Conf. Soil Mech. and Found. Eng., Vol. 1, 1953, pp. 238-251.
6) E.C.W.A. Geuze : Compression, an Important Facter in the Shearing Test, Proc. 2nd Int. Conf. Soil Mech. and Found. Eng., Vol. 3, 1948, pp. 139-142.
7) S.S. Vialov and A.M. Skibitsky : Rheological Process in Frozen Soil and Dense Clays, Proc. 4th Int. Conf. Soil Mech. and Found. Eng., Vol. 1, 1957, pp. 120-124.
8) E.C.W.A. Geuze and T.K. Tan . The Mechanical Behaviour of clays, Proc. 2nd Int. Cong. Rheol., pp. 247-259.
9) A. Yoshimoto : An experimental Study on the Deformation of Concrete, J. S. C. E., Vol. 40, No. 9, 1955, pp. 22-27.
10) S. Murayama, K. Akai and T. Shibata : The Effect of the Moisture Content on the Strength of an Alluvial Clay, Disaster Prevention Research Inst. Kyoto Univ. Bulletin No. 12, Dec., 1955.
11) M. Goldstein and G.T. Stepanian : The Long-term Strength of Clays and Depth Creep of Slopes, Proc. 4th Int. Conf. Soil Mech. and Found. Eng., Vol. 2, 1957, pp. 311-314.
12) A. Casagrande and D. Wilson : Effect of Rate of Loading on the Strength of Clays and Shales at Constant Water Content, Harvard Soil Mech. Series, No. 39, Cambridge, Mass., 1950.

Publications of the Disaster Prevention Research Institute

The Disaster Prevention Research Institute publishes reports of the research results in the form of bulletins. Publications not out of print may be obtained free of charge upon request to the Director, Disaster Prevention Research Institute, Kyoto University, Kyoto, Japan.

Bulletins :

No. 1 On the Propagation of Flood Waves by Shoitiro Hayami, 1951.
No. 2 On the Effect of Sand Storm in Controlling the Mouth of the Kiku River by Tojiro Ishihara and Yuichi Iwagaki, 1952.
No. 3 Observation of Tidal Strain of the Earth (Part I) by Kenzo Sassa, Izuo Ozawa and Soji Yoshikawa. And Observation of Tidal Strain of the Earth by the Extensometer (Part II) by Izuo Ozawa, 1952.
No. 4 Earthquake Damages and Elastic Properties of the Ground by Ryo Tanabashi and Hatsuo Ishizaki, 1953.
No. 5 Some Studies on Beach Erosions by Shoitiro Hayami, Tojiro Ishihara and Yuichi Iwagaki, 1953.
No. 6 Study on Some Phenomena Foretelling the Occurrence of Destructive Earthquakes by Eiichi Nishimura, 1953.
No. 7 Vibration Problems of Skyscraper. Destructive Element of Seismic Waves for Structures by Ryo Tanabashi, Takuzi Kobori and Kiyoshi Kaneta, 1954.
No. 8 Studies on the Failure and the Settlement of Foundations by Sakurō Murayama, 1954.
No. 9 Experimental Studies on Meteorological Tsunamis Traveling up the Rivers and Canals in Osaka City by Shoitiro Hayami, Katsumasa Yano, Shohei Adachi and Hideaki Kunishi, 1955.
No.10 Fundamental Studies on the Runoff Analysis by Characteristics by Yuichi Iwagaki, 1955.
No.11 Fundamental Considerations on the Earthquake Resistant Properties of the Earth Dam by Motohiro Hatanaka, 1955.
No.12 The Effect of the Moisture Content on the Strength of an Alluvial Clay by Sakurō Murayama, Kōichi Akai and Tōru Shibata, 1955.
No.13 On Phenomena Forerunning Earthquakes by Kenzo Sassa and Eiichi Nishimura, 1956.
No.14 A Theoretical Study on Differential Settlements of Structures by Yoshitsura Yokoo and Kunio Yamagata, 1956.
No.15 Study on Elastic Strain of the Ground in Earth Tides by Izuo Ozawa, 1957.
No.16 Consideration on the Mechanism of Structural Cracking of Reinforced Concrete Buildings Due to Concrete Shrinkage by Yoshitsura Yokoo and S. Tsunoda, 1957.
No.17 On the Stress Analysis and the Stability Computation of Earth Embankments by Kōichi Akai, 1957.
No.18 On the Numerical Solutions of Harmonic, Biharmonic and Similar Equations by the Difference Method Not through Successive Approximations by Hatsuo Ishizaki, 1957.
No.19 On the Application of the Unit Hydrograph Method to Runoff Analysis for Rivers in Japan by Tojiro Ishihara and Akiharu Kanamaru, 1958.
No.20 Analysis of Statically Indeterminate Structures in the Ultimate State by Ryo Tanabashi, 1958.
No.21 The Propagation of Waves near Explosion and Fracture of Rock (I) by Soji Yoshikawa, 1958.
No.22 On the Second Volcanic Micro-Tremor at the Volcano Aso by Michiyasu Shima, 1958.
No.23 On the Observation of the Crustal Deformation and Meteorological Effect on It at Ide Observatory and on the Crustal Deformation Due to Full Water and Accumulating Sand in the Sabo-Dam by Michio Takada, 1958.
No.24 On the Character of Seepage Water and Their Effect on the Stability of Earth Embankments by Kōichi Akai, 1958.
No.25 On the Thermoelasticity in the Semi-infinite Elastic Soid by Michiyasu Shima
No.26 On the Rheological Characters of Clay (Part 1) by Sakurō Murayama and Tōru Shibata, 1958.

Bulletin No. 26 Published October, 1958

昭和 33 年 10 月 15 日 印 刷
昭和 33 年 10 月 20 日 発 行

編輯兼発行者 京都大学防災研究所
印刷者 山 代 多 三 郎
京都市上京区寺之内通小川西入
印刷所 山代印刷株式会社